

NASA TM X-9

NASA TM X-9



IN 07  
380403

# TECHNICAL MEMORANDUM

X-9

INVESTIGATION OF THE EFFECTS OF LOW REYNOLDS NUMBER  
OPERATION ON THE PERFORMANCE OF A SINGLE-STAGE  
TURBINE WITH A DOWNSTREAM STATOR

By Robert E. Forrette, Donald E. Holeski, and Henry W. Plohr

Lewis Research Center  
Cleveland, Ohio

Declassified April 23, 1962

NATIONAL AERONAUTICS AND SPACE ADMINISTRATION  
WASHINGTON

September 1959



NATIONAL AERONAUTICS AND SPACE ADMINISTRATION

---

TECHNICAL MEMORANDUM X-9

---

INVESTIGATION OF THE EFFECTS OF LOW REYNOLDS NUMBER OPERATION ON THE  
PERFORMANCE OF A SINGLE-STAGE TURBINE WITH A DOWNSTREAM STATOR

By Robert E. Forrette, Donald E. Holeski, and Henry W. Flohr

SUMMARY

High-altitude turbojet performance is adversely affected by the effects of low air density. This performance loss is evaluated as a Reynolds number effect, which represents the increased significance of high fluid viscous forces in relation to dynamic fluid forces as the Reynolds number is decreased.

An analytical and experimental investigation of the effects of low Reynolds number operation on a single-stage, high-work-output turbine with a downstream stator was carried out at Reynolds numbers of 182,500, 39,600, and 23,000, based on average rotor-design flow conditions.

At low Reynolds numbers and turbulent flow conditions, increased viscous losses caused decreased effective flow area, and thus decreased weight flow, torque, and over-all efficiency at a given equivalent speed and pressure ratio.

Decreasing the Reynolds number from 182,500 to 23,000 at design equivalent speed resulted in a 5.00-point loss in peak over-all turbine efficiency for both theory and experiment. The choking equivalent weight flow decreased 2.30 percent for these conditions.

Limiting loading work output was reached at design equivalent speed for all three Reynolds numbers. The value of limiting loading work output at design speed decreased 4.00 percent as Reynolds number was decreased from 182,500 to 23,000.

A theoretical performance-prediction method using basic boundary-layer relations gave good agreement with experimental results over most

of the performance range at a given Reynolds number if the experimental and analytical design operating conditions were carefully matched at the highest Reynolds number with regard to design performance parameters.

High viscous losses in the inlet stator and rotor prevented the attainment of design equivalent work output at the lowest Reynolds number of 23,000.

## INTRODUCTION

In the operation of turbojet engines at high altitudes, the performance of the compressor and turbine components is adversely affected by the effects of the low air density. The higher losses at these conditions are caused by the relatively increased effect of the viscous forces on the fluid flow as the dynamic forces are decreased because of the lower air density. The fluid Reynolds number, which is the ratio of the dynamic to the viscous forces in the fluid, is the significant parameter in evaluating these performance changes.

The performance of the compressor component of turbojet engines operating under simulated altitude conditions is reported in references 1 and 2. The results of fundamental single- and multistage component investigations are described in references 3 to 5. These investigations have indicated a fairly well-defined depreciation in compressor performance as the fluid Reynolds number is reduced. Similar investigations of turbine performance when the turbine is operating as part of a complete engine have not yielded such definite results. The results presented in reference 2 indicate that some of the engines investigated had a reduction in turbine efficiency for the lowest Reynolds number level investigated. No change in turbine equivalent weight flow was detected. In reference 2 it is indicated that the efficiency change noted was partially due to a shift in the turbine operating point. This type of experimental difficulty can be avoided if the turbine performance is obtained in a turbine-component test facility. Such a facility also yields more detailed information over a wider operating range, and it is easier to maintain the necessary high experimental accuracy. In some cases, investigations of this type over a limiting range of Reynolds number (refs. 6 and 7) have not indicated any measurable change in turbine performance. Other investigations (refs. 2 and 8) clearly demonstrated a fluid Reynolds number effect on turbine efficiency but did not demonstrate a change in turbine equivalent weight flow.

Experimental evaluation of the performance of a turbine operating over a range of fluid Reynolds number is of great value if the performance evaluation is related to the fundamental understanding of fluid flow in turbomachinery. It has been common practice to correlate the

efficiency of compressors by expressing the over-all loss as an exponential function of the fluid Reynolds number (refs. 1, 3, 4, and 5). A correlation of this type is based on the assumption that the change in the loss is due entirely to a change in fluid viscous loss and therefore depends only on fluid Reynolds number. This assumption is probably valid for both compressors and turbines if the correlation of loss (and, hence, efficiency) is based on the minimum loss (hence, maximum efficiency) for equivalent operating points. However, the operating point for the peak efficiency will probably shift slightly with fluid Reynolds number level, thereby making an accurate correlation impossible by this method. In order to provide a more complete understanding of the experimental data, it is necessary to use a more complex analytical approach that will account for the change in viscous loss with changes in fluid Reynolds number, the interaction of this change in loss with other turbine losses, and also the change in turbine operating point.

The performance characteristics of an experimental single-stage turbine having a downstream stator were obtained in a turbine-component test facility. The fluid Reynolds number was changed by changing the pressure level in the facility. Complete performance data were obtained over a range of blade speed and pressure ratio at three pressure levels corresponding to rotor-chord Reynolds numbers of 23,000, 39,600, and 182,500. The lowest Reynolds number of 23,000 would correspond approximately to that of a turbine operating in an engine with a compressor pressure ratio of 6.0 at 100-percent design speed and a turbine-inlet temperature of 2500° R, at a flight Mach number of 1.5 and a 95,000-foot altitude.

In order to relate fundamental concepts of viscous fluid flow with observed changes in turbine performance, an analytical turbine-performance calculation technique was utilized. This technique made use of experimentally determined performance at a given fluid Reynolds number level in order to establish the turbine viscous loss coefficients. These loss coefficients were then assumed to change with fluid Reynolds number in a manner corresponding to turbulent flat-plate friction losses. The performance analysis was then used to evaluate the turbine performance over a range of pressure ratio and blade speed at Reynolds number levels corresponding to those investigated experimentally. The results of this analysis are compared with the experimentally determined performance.

#### SYMBOLS

$A_t$  frontal area, sq ft

$a_{cr}$  critical velocity,  $\sqrt{\frac{2r}{r+1}} gRT$

$C$  constant

g	gravitational constant, 32.174, ft/sec <sup>2</sup>
H	boundary-layer form factor, $\delta^*/\theta^*$
$\Delta h$	turbine work, Btu/lb
L	loss parameter, $\frac{1 - \eta}{\eta} / \left( \frac{1 - \eta}{\eta} \right)_{\text{ref}}$
P	total pressure, lb/sq ft
p	static pressure, lb/sq ft
R	gas constant, 53.35 ft-lb/(lb)(°R)
Re	Reynolds number
s	blade spacing, ft
T	total temperature, °R
t	trailing-edge thickness, ft
U	blade speed, ft/sec
$\sqrt{u^2}$	root-mean-square longitudinal component of turbulent perturbation velocity, ft/sec
V	absolute velocity, ft/sec
w	weight flow, lb/sec
x	flat-plate coordinate
$\alpha$	absolute flow angle, angle between velocity and axial direction, deg
$\gamma$	ratio of specific heats
$\delta$	ratio of total pressure to NASA standard sea-level pressure of 2116 lb/sq ft
$\delta^*$	displacement thickness

$$\epsilon \quad \text{function of } \gamma, \frac{r_{sl}}{r} \left[ \frac{\left(\frac{\gamma+1}{2}\right)^{\frac{\gamma}{\gamma-1}}}{\frac{r_{sl}}{r_{sl}^{-1}}} \right]$$

$\eta$  adiabatic efficiency

$\theta_{cr}$  squared ratio of critical velocity to critical velocity at NASA standard conditions

$\theta^*$  boundary-layer momentum thickness, ft

$\lambda$  blade viscous-loss parameter

$\rho$  gas density, lb/cu ft

$\tau$  torque, ft-lb

#### Subscripts:

ac actual value

av average value

cr critical value

e blade exit, trailing-edge plane

fs free-stream value between blade wakes

id ideal value

in station at inlet to a blade row

L loss value

m station after complete mixing occurs

n station just downstream of blade row

ref reference value (Reynolds number, 182,500)

sl NASA sea-level standard conditions ( $T_{sl} = 518.7^\circ \text{ R}$ )

T	absolute total state
t	tip
x	flat-plate coordinate
z	axial component or direction
1,2, 3,4	measuring stations (see fig. 1)

## APPARATUS AND PROCEDURE

### Test Facility and Instrumentation

The 15-inch-tip-diameter turbine-component test facility described in reference 9 was used in this investigation. A schematic diagram of the installation is shown in figure 1. Ambient air was filtered in an electrostatic precipitator and then heated to 225° F in order to avoid the possibility of forming condensation shocks downstream of the turbine. The airflow was measured by a calibrated ASME flat-plate orifice. Three orifices of different diameters were used over the range of Reynolds numbers in order to maintain high measurement accuracy. After passing through the turbine test section, the air was exhausted to the laboratory altitude exhaust system.

The power output of the turbine was absorbed by either of two eddy-current-type, cradle-mounted dynamometers. One of these had a power absorption capacity of 125 horsepower and was used for tests at the low Reynolds numbers. The larger dynamometer had a 1700-horsepower capacity and was used at the high Reynolds number condition.

Rotor speed was measured with an electronic speed counter that registered the measured rotative speed to an accuracy of 1 rpm.

The turbulence in the airstream at the turbine inlet was measured by a constant-temperature-type hot-wire anemometer of the same configuration as described in appendix B and figure 16(b) of reference 10.

The circumferential and axial locations of static-pressure taps, total-pressure and thermocouple probes, and the self-balancing, angle-positioning probe actuators used in measuring flow angles are shown schematically in figure 1(b). The instrumentation is the same as that of reference 9 with the exception that manometer fluids of lower specific



gravity were used to measure the lower pressures. This allowed a higher accuracy of measurement than is possible with the heavier fluids commonly used.

The model turbine used in the experimental investigation was a single-stage, high-work-output type which incorporated a downstream stator for recovery of energy contained in the whirl component of velocity at the rotor exit. The turbine was of the same design as that described in reference 9, except that a rotor-tip-clearance recess in the outer annulus wall was filled, and the rotor-tip radius decreased proportionately in order to maintain suitable clearance between the rotor tip and the wall.

### Experimental Procedure

Experimental data were recorded over a range of speed and pressure ratio at each of three Reynolds numbers in order to obtain a complete turbine performance map at each Reynolds number. The inlet total pressure was set at approximately 2.90, 5.00, and 23.00 inches of mercury absolute in order to obtain turbine design point Reynolds numbers of 23,000, 39,600, and 182,500, respectively, based on rotor mean chord and design relative flow conditions averaged between the rotor-inlet and exit mean radius values. The inlet total temperature was kept constant at 685° R.

The friction torque of the bearings on the turbine shaft was measured over a range of shaft speeds in a separate test. This torque was added to the dynamometer measured torque in order to calculate the aerodynamic output torque of the experimental turbine. The torque absorbed by the bearings was about 2 percent of the over-all torque at design speed and pressure ratio for the lowest inlet pressure investigated.

The turbulence intensity at the turbine inlet was measured by radial hot-wire surveys at inlet pressures of approximately 25 and 5 inches of mercury absolute.

Surveys of the flow conditions at the stator inlet indicated that a large temperature gradient existed when the facility was operated with low plenum pressures. Proper insulation of the inlet piping and plenum reduced this gradient to an acceptable level.

### Experimental Data Reduction and Performance Calculations

The method of calculating and presenting the turbine performance data was the same as that of reference 9. The total pressure at a station, as calculated by equation (1) of reference 9, is a function of

static pressure, total temperature, weight flow, and flow angle. The rating total pressure at a station is defined as the static pressure at that station plus the dynamic pressure contributed by the axial component of velocity. The rating total pressure is calculated by using equation (2) of reference 9.

The experimental torque and weight flow data were plotted against over-all rating total-pressure ratio for lines of constant equivalent blade speed at each of the three Reynolds numbers investigated. These data were faired and used to develop performance maps at each Reynolds number in the same manner as in reference 9. The over-all turbine efficiency was obtained from blade speed, weight flow, aerodynamic torque, and the ideal work, which was determined from the calculated pressure ratio. The aerodynamic equivalent torque was obtained by correcting the dynamometer measurement for bearing friction.

The intensity of free-stream turbulence is important in correlating experimental results obtained in a given test installation with those obtained in others over a range of Reynolds numbers. It is also significant in considering to what extent the boundary layer is laminar on the blade surfaces. The intensity of turbulence is represented by a param-

eter  $\frac{\sqrt{u^2}}{v}$  which is defined as the root-mean-square of the turbulent perturbation velocity divided by the free-stream velocity. The parameter expresses turbulence as a percentage of the free-stream velocity and was calculated from hot-wire voltage measurements using equation (B1) of reference 10. The average intensity of turbulence in the inlet annulus was approximately 4 percent of the mean free-stream velocity at the low pressure and 1.75 percent at the high pressure. These values are relatively high compared with those of the order of 0.1 percent and less that exist in low turbulence wind tunnels (ref. 11), but are probably low when compared with the intensity of turbulence in the high-temperature gas flow of an actual engine.

#### Analytical Performance Prediction Method

The method of analytical performance prediction is similar to that of references 12 and 13. Various loss assumptions, the continuity equation, and basic one-dimensional flow equations are used to compute parameters which define the flow conditions at the mean radius between blade rows. These parameters are then used to calculate over-all work, efficiency, and weight flow. The loss assumptions include the following:

Blade viscous loss. - This includes all viscous losses in the boundary layer on the blade surfaces and annulus walls, and any losses caused

by secondary flows, tip clearances, and shock waves. The blade viscous loss is represented by a parameter  $\lambda$ , which is defined as a kinetic-energy-loss coefficient in order to relate the viscous loss with velocity parameters. The parameter  $\lambda$  is expressed as a function of average kinetic-energy loss relative to a given blade row by equation (A7) in the appendix. Total-pressure losses obtained from experimental surveys of the upstream stator at design flow conditions were used in conjunction with the experimental turbine efficiency at design work and blade speed to estimate the total-pressure losses for each blade row. These losses, determined experimentally at the high Reynolds number operating condition, were used to calculate the blade loss parameter for each blade row. The values of  $\lambda$  were held fixed in computing the turbine off-design performance at a given Reynolds number level. This viscous loss parameter was used in preference to that employed in references 12 and 13 because better agreement was obtained between the predicted turbine off-design performance and the experimental performance obtained at the high Reynolds number level.

Inlet-angle loss. - For the rotor and downstream stator another component of the total loss is the inlet-angle loss. This loss is defined as that due to deviation of direction of the blade-inlet velocity vector from the design value. The loss is thus equal to zero at design conditions. At off-design conditions the inlet velocity vector is resolved into components normal and parallel to the original design vector, and the normal component is assumed lost. This corresponds to the incidence loss assumption of references 12 and 13.

Exit whirl loss. - For the  $\frac{1}{2}$ -stage turbine it is assumed that the downstream stator always turns the flow to the axial direction so that the exit whirl loss is zero for purposes of over-all efficiency calculation.

Loss variation with Reynolds number. - In order to calculate the predicted variation of turbine performance with fluid Reynolds number, the experimentally determined values of the blade viscous loss parameter  $\lambda$  that were used in calculating the off-design performance at the high Reynolds number were modified in the following way.

The variation of  $\lambda$  with Reynolds number is obtained by using the Prandtl 1/5th-power law for the turbulent boundary layer over the range of Reynolds number considered. The Prandtl relation is:

$$\frac{\theta^*}{x} = C(\text{Re}_x)^{-1/5} \quad (1)$$

This equation was derived for a 1/7th-power velocity profile in the turbulent boundary layer on a flat plate with zero pressure gradient (ref. 14).

The value of  $\lambda$  at a given reference Reynolds number taken at the design operating point is obtained from equation (A7) of the appendix using design values of velocity ratio and calculated total-pressure loss. In order to calculate  $\lambda$  for any other Reynolds numbers, the following procedure is used:

(1) The momentum thickness  $\theta_{\text{ref}}^*$  for the given reference Reynolds number is calculated using equations (A8) and (A9) of the appendix in an iterative procedure.

(2) The momentum thickness  $\theta^*$  for the desired Reynolds number is calculated using equation (A10).

(3) The pressure ratio  $P_2/P_1$  is calculated using equations (A8) and (A9) of the appendix.

(4) The value of the loss parameter  $\lambda$  corresponding to the desired Reynolds number may then be calculated from equation (A7) of the appendix. The derivation of the parameter  $\lambda$  and a more detailed discussion of its variation with Reynolds number is given in the appendix.

The calculated values of  $\lambda$  and the associated total-pressure losses of each blade row (assuming design mean-radius flow conditions for each blade row) for the three Reynolds numbers are tabulated in the following table:

	Inlet stator	Rotor	Downstream stator
Reynolds number, 182,500			
Loss total-pressure ratio <sup>a</sup>	0.9750	0.8943	0.9849
Loss parameter, $\lambda$	.0779	.1867	.0423
Reynolds number, 39,600			
Loss total-pressure ratio	0.9664	0.8594	0.9797
Loss parameter, $\lambda$	.1059	.2518	.0577
Reynolds number, 23,000			
Loss total-pressure ratio	0.9626	0.8441	0.9774
Loss parameter, $\lambda$	.1182	.2808	.0634

<sup>a</sup> Ratio of blade-exit relative total pressure to the inlet value.

## RESULTS AND DISCUSSION

In evaluating the change in performance of a turbine over a range of Reynolds numbers it is important to determine, if possible, the change in flow conditions occurring in each blade row. This is especially true for the turbine of the present investigation because it has a downstream stator. The flow conditions in the downstream stator may be particularly sensitive to the effects of low fluid Reynolds numbers because of the adverse pressure gradient through this blade row. Consequently, the change in performance of the downstream stator with Reynolds number may have a dominating influence on the over-all performance of the turbine at low Reynolds numbers.

The over-all turbine performance at three different Reynolds numbers is presented first. The performance results are then correlated with the information obtained from interstage measurements in order to determine the effect of Reynolds number changes on the performance of individual blade rows.

### Over-All Performance

The complete performance of the turbine at three Reynolds numbers is presented in figure 2. The map is a plot of the equivalent turbine work  $\frac{\Delta h}{\theta_{cr}}$  as a function of the weight-flow-speed parameter  $wU_t \epsilon / A_t \delta_1$ , for lines of constant rating total-pressure ratio  $P_1/P_{z,4}$  and equivalent blade speed  $\frac{U_t}{\sqrt{\theta_{cr}}}$ . The over-all rating efficiency  $\eta_{z,4}$  is shown in the form of contours on the map.

The variations of equivalent aerodynamic torque  $\frac{\tau}{\delta} \epsilon$  and equivalent weight flow  $\frac{w\sqrt{\theta_{cr}}}{\delta_1} \epsilon$  with over-all rating total-pressure ratio  $P_1/P_{z,4}$  for the three Reynolds numbers are shown in figures 3 and 4, respectively. Actual data points are plotted on the figures, and values read from the faired curves were used in calculating the performance maps of figure 2.

The variation of the absolute flow angle at the downstream stator exit (station 4) with equivalent work is shown in figure 5. The plotted points are radial averages of individual probes at different circumferential positions at station 4.

The effect of Reynolds number on over-all performance can be illustrated by examining the variations of choking equivalent weight flow,

peak efficiency, and maximum equivalent work at design speed as Reynolds number varies from 182,500 to 23,000. The maps of figure 2 and the weight-flow curves of figure 4 show a decrease of 2.30 percent in the value of the choking equivalent weight flow over the range of Reynolds numbers at design speed. The maps also show a decrease of approximately 5 points in the peak efficiency and a decrease of 4.00 percent in the maximum work output at design speed as the Reynolds number was reduced from 182,500 to 23,000.

In evaluating the extent to which flow variations in the downstream stator affected the changes in over-all turbine performance, it is desirable to determine the performance of the first two blade rows independently. However, this was prevented by difficulties in obtaining accurate measurements of rotor-exit flow angle at low Reynolds numbers. A discussion showing that the change in Reynolds number affects the flow conditions in both the first stator and the rotor through consideration of the turbine choking flow characteristics of individual blade rows is presented in the following section.

#### Blade-Row Performance

At the low blade speeds (60- and 70-percent design) the weight flow curves of figure 4 show that the inlet stator is choked because the choking equivalent weight flow is unchanged with blade speed. At this condition the choking equivalent weight flow is reduced 1.30 percent as the Reynolds number is decreased from 182,500 to 39,600 (figs. 4(a) and (b)). Apparently the stator effective flow area is reduced by this amount because of the increased boundary-layer displacement thicknesses in the stator as the Reynolds number is reduced.

At rotor speeds from 80- to 120-percent design, the choking equivalent weight flow at a given Reynolds number varies with blade speed, indicating choking either in the rotor or downstream stator (fig. 4). At design blade speed, the rotor blades are designed to choke at a pressure ratio less than that required to choke the downstream stator. As the over-all pressure ratio is increased beyond that required to choke the rotor blades, the rotor should reach limiting loading work output, and then choking should occur in the downstream stator. However, because of possible errors in blade fabrication, or in blade-loss estimation used in the design procedure, the downstream stator may choke at some over-all pressure ratio lower than that at which the rotor reaches limiting loadings. In this case the maximum work output of the turbine is limited by choking in the downstream stator. In order to determine whether this occurred in the subject turbine, the ratio of static pressure at a given axial station to the inlet total pressure is plotted as a function of over-all pressure ratio in figure 6. If, for a given over-all pressure ratio, the curve for a given station has a definite

slope, while the curve for the preceding station has zero slope, the blade row between those stations is choking. The values of over-all pressure ratio at design speed for rotor choking, maximum work, and downstream stator choking are summarized in the following table:

Reynolds number	Approximate over-all pressure ratio ( $P_1/P_{4,z}$ ) at design speed		
	Rotor choking	Maximum work	Downstream stator choking
182,500	2.2	2.5	2.5
39,600	2.3	2.6	2.6
23,000	2.3	2.6	2.7

The ratios  $P_1/P_{z,4}$  for rotor choking and that for downstream stator choking were estimated from the curves of figure 6. The ratio for maximum work was obtained from the design-speed torque curve of figure 3 where the curve slope is initially zero.

According to the values of pressure ratio in the above table, the turbine either reached limiting loading work output at approximately the same pressure ratio as that at which the downstream stator choked, or downstream stator choking is limiting the turbine work output. The differences in the values of pressure ratio obtained from figures 3 and 6 are too small to provide a definite conclusion of the occurrence of limiting loading except at the lowest Reynolds number. According to figure 3(c), the over-all pressure ratio at limiting loading work was 2.61 at design speed for the Reynolds number of 23,000. The downstream stator did not choke till a higher pressure ratio was reached, as indicated in figure 6(c). Thus, it is concluded that the rotor reached limiting loading work at the lowest Reynolds number. According to reference 9 it was shown that limiting loading work was attained at all but the 110- and 120-percent design blade speeds. Although the turbine of the present discussion differed from that of reference 9 by the removal of the tip clearance recess from the outer wall, the performance results were practically identical. It is thus concluded that the subject turbine reached limiting loading work at the highest Reynolds number. Since it has also been shown that the turbine reached limiting loading at the lowest Reynolds number (23,000), it may be concluded that the turbine also reached limiting loading at all intermediate Reynolds numbers.

A qualitative estimate of the effect of low fluid Reynolds number operation on rotor performance can be seen by examining the weight-flow

curves of figure 4 and the choking pressure ratios in the preceding table (p. 13). From figure 4 it can be concluded that, for a constant blade speed and pressure ratio, the choking equivalent weight flow decreases in value as Reynolds number is decreased. If, at design speed, a value of pressure ratio between that for initial rotor choking and that for downstream stator choking (table, p. 13) is chosen, the decrease in weight flow with Reynolds number at this pressure ratio indicates that the effect of lower fluid Reynolds number on the rotor is to decrease the choking weight flow through the rotor as Reynolds number decreases. It is concluded that either the rotor or inlet-stator effective flow area is reduced because of increased viscous losses upstream of the rotor throat as the Reynolds number is decreased to the lower values.

The equivalent design work at design speed was not obtained at the lowest Reynolds number (23,000), as indicated in figure 2(c). The curves of figure 2 show a decrease of 4 percent in the experimental value of maximum rotor work at design speed as the Reynolds number changes from 182,500 to 23,000. The 4-percent decrease in experimental maximum work is probably due to a combination of decreased rotor-inlet and exit whirl resulting from increased inlet stator and rotor viscous losses. It may be concluded that a combination of high viscous losses in both the rotor and inlet stator prevented the turbine from delivering design work output at the lowest Reynolds number.

#### Over-All Loss Variation With Reynolds Number

The enthalpy changes through the turbine can be expressed as

$$\Delta h_{ac} = \Delta h_{id} - \Delta h_L \quad (2)$$

and the efficiency as

$$\eta = \frac{\Delta h_{ac}}{\Delta h_{id}} \quad (3)$$

A combination of equations (2) and (3) gives

$$\frac{1 - \eta}{\eta} = \frac{\Delta h_L}{\Delta h_{ac}} \quad (4)$$

The term  $\frac{1 - \eta}{\eta}$  is then the ratio of the enthalpy loss to the total enthalpy drop through the turbine. If this loss parameter is assumed to represent a momentum loss due to viscous friction, it can be considered proportional to the boundary-layer momentum thickness on the blade surfaces and annulus walls within the turbine. The variation of this loss parameter with Reynolds number at a given rotor speed and constant actual



work output is then an indication of the change in viscous loss with Reynolds number and may be expressed by equation (1) as

$$L = \frac{\frac{1 - \eta}{\eta}}{\left(\frac{1 - \eta}{\eta}\right)_{\text{ref}}} = \left(\frac{\text{Re}_{\text{ref}}}{\text{Re}}\right)^{1/5} \quad (5)$$

where the highest Reynolds number is used as a reference value. The theoretical variation of the over-all turbine loss parameter  $L$  is then shown in figure 7 as a straight line using the reference Reynolds number as 182,500.

In figure 8(c) the peak efficiency for each of the three Reynolds numbers at design rotor speed occurs at a work output of approximately 16.00 Btu per pound. At this point most of the change in over-all loss is due to changes in viscous loss. The values of over-all efficiency  $\eta_{z,4}$  at the peak efficiency points were used to calculate the over-all turbine loss parameter  $L_4$  at each Reynolds number. These experimental values of loss parameter are shown in figure 7.

The slope of the experimental curve appears to flatten as the Reynolds number ratio approaches 1.0 (fig. 7), corresponding to a Reynolds number of 182,500. This trend also occurred for loss as a function of Reynolds number in the compressor-stage investigation of reference 1, which indicated that a constant value of momentum loss exists at Reynolds numbers of approximately 200,000 and higher. This is probably caused by the effect of blade surface roughness. For relatively high Reynolds numbers the laminar sublayer of the turbulent boundary layer becomes very thin, and the average blade-surface-roughness height is then the controlling influence on viscous losses.

In the compressor investigation of reference 5 loss variations were recorded which correlated well with laminar boundary-layer theory at low Reynolds numbers. The critical Reynolds number for transition from laminar to turbulent flow occurred at a value corresponding to approximately 0.18 on the abscissa of figure 7. In the present investigation the low Reynolds number loss variation closely approximates the variation specified by turbulent boundary-layer theory, and no apparent transition was observed. This is probably due principally to the relatively high value of free-stream turbulence intensity (4 percent) at the turbine inlet. The high free-stream turbulence would induce transition from laminar to turbulent boundary-layer flow on the blade surfaces at a chordwise position close to the blade leading edge, so that the boundary layer is turbulent over most of the blade surface.

At the Reynolds numbers investigated, the theoretical loss variations based on the relation of equation (5) are in good qualitative agreement with the experimental results. Thus the 1/5th-power law is a good qualitative approximation for estimating over-all turbine loss variations with Reynolds number if the Reynolds numbers are low.

#### Theoretical and Experimental Reynolds Number Effects

The Prandtl 1/5th-power law for the turbulent boundary layer was used as outlined in the appendix in estimating the variation of viscous loss with Reynolds number. Fundamental boundary-layer relations were used to estimate blade viscous losses at a given Reynolds number. These procedures gave satisfactory results when used as part of the performance prediction method for calculating theoretical turbine performance for the range of Reynolds numbers.

In figure 8 the Reynolds number effect on the over-all turbine efficiency  $\eta_{z,4}$  is shown for speeds ranging from 80 to 120 percent of design. Both experimental and theoretical values are shown. Good agreement between the theoretical and experimental curves is observed except at the high and low extremes of work output. Theoretical values of limiting loading work are low except at the two highest speeds. Differences between theoretical and experimental curves must be attributed to the difficulty of calculating blade losses accurately at off-design conditions. However, for most of the performance range, the method of performance prediction is considered to be an effective means of estimating turbine performance.

At design speed the peak efficiency decrease with Reynolds number at an equivalent work of 16.00 Btu per pound is 5.00 points for both theory and experiment.

Even though the ability of the performance prediction method to calculate the absolute magnitude of the choking weight flow and maximum turbine work output is not completely satisfactory, it is a very effective means of predicting the changes in choking weight flow and maximum work output over a range of Reynolds numbers. The variation of the ratio of the choking weight flow over a range of Reynolds numbers divided by the choking weight flow at the reference Reynolds number is shown in figure 9 for both the experimental data and the performance prediction method. Also figure 10 shows the variation of the ratio of maximum turbine work output over a range of Reynolds numbers divided by the maximum turbine work output at the reference Reynolds number for both the experimental data and the performance prediction method.

The decrease in over-all efficiency from the highest Reynolds number of 182,500 to the low Reynolds numbers of 39,600 and 23,000 is presented in terms of an efficiency difference as a function of turbine work at design speed in figure 11. Experimental and theoretically predicted curves are presented for each of the low Reynolds numbers. The agreement between experimental and predicted efficiency difference is better for the lowest Reynolds number (23,000) over the entire range of work output than for the Reynolds number of 39,600. For both of the low Reynolds numbers the predicted change in efficiency agrees best with the experimental value in the region of peak efficiency ( $\Delta h/\theta_{cr} = 16.00$  Btu/lb).

The simple 1/5th-power relation of equation (5) was used to calculate the efficiency change points at a work output of 16.00 Btu per pound where the viscous losses predominate. These points are plotted for both Reynolds numbers as shown in figure 11, and show that the simple 1/5th-power relation is a fairly good approximation for efficiency change with Reynolds number in the region of peak efficiency at design speed. The points shown differ from the experimental values by 1.20 and 0.70 percent for the Reynolds numbers of 39,600 and 23,000, respectively.

In general, it is concluded that the theoretical performance prediction method used along with boundary-layer relations is a good approximation at a given Reynolds number if the reference Reynolds number parameters are calculated using design velocity diagrams and accurate values of blade losses at the design operating condition.

#### Loss Analysis

A breakdown of the various blade losses calculated as part of the theoretical performance prediction method for the Reynolds numbers of 182,500 and 23,000 is shown in figure 12. The losses due to incidence angle and the viscous blade loss are shown as consecutive decreases in efficiency between the curves over the range of turbine work output at design speed. The lowest curve is the theoretical over-all efficiency  $\eta_{z,4}$ . For both Reynolds numbers the viscous blade loss is the major portion of the total loss, especially at high work outputs near the design value of 22.31 Btu per pound.

As the Reynolds number is decreased from 182,500 to 23,000, the theoretical rotor viscous losses increase so that approximately 3 to 5 additional points in efficiency are lost, depending on the work output.

At the lower Reynolds number the theoretical viscous losses in each blade row were greater than those at the high Reynolds number, as is shown by the increased displacements between the curves.

For each Reynolds number at design speed, the incidence losses are significant only at the lower values of work output.

#### SUMMARY OF RESULTS

1. Experimental investigation and analysis of the performance of a turbine over a wide range of Reynolds numbers showed that losses increased with decreasing Reynolds numbers, which caused reductions in flow, torque, and efficiency at a given equivalent speed and pressure ratio. The analysis showed that for the turbine discussed herein the changes in turbine performance near design operating conditions were due primarily to a simple increase in the turbulent boundary-layer losses on the blade in accordance with the Prandtl  $1/5$ th-power-law variations. Changes in incidence and secondary flow effects with Reynolds number were not significant.

2. At design speed the measured peak over-all turbine efficiency decreased 5.00 points for both theory and experiment as Reynolds number decreased from 182,500 to 23,000.

3. The choking equivalent weight flow decreased 2.30 percent as Reynolds number decreased from 182,500 to 23,000. The location of choking in the turbine was the same for all Reynolds numbers at design speed.

4. The data indicated that the rotor reached limiting loading work output at design speed at all three Reynolds numbers. The limiting loading work output at design speed decreased 4.00 percent as Reynolds number was reduced from 182,500 to 23,000.

5. The theoretical performance calculation method employing fundamental boundary-layer relations provided a good approximation of turbine performance at a given Reynolds number if the reference Reynolds number parameters are calculated using design velocity diagrams and accurate values of blade losses at the design operating condition.

6. Design equivalent work was not obtained at the lowest Reynolds number (23,000) because of high viscous losses in the inlet stator and the rotor.

Lewis Research Center  
National Aeronautics and Space Administration  
Cleveland, Ohio, February 12, 1959

## APPENDIX - BLADE LOSS PARAMETER AND VARIATION WITH REYNOLDS NUMBER

## Loss Coefficients and Boundary-Layer Parameters

The kinetic-energy loss due to friction may be represented by a coefficient  $\lambda$  which is the lost portion of the average kinetic energy contained in the average velocity across a blade row. The average velocity is defined as

$$\left(\frac{V}{a_{cr}}\right)_{av} = \sqrt{\frac{1}{2} \left[ \left(\frac{V_{in}}{a_{cr}}\right)^2 + \left(\frac{V_e}{a_{cr}}\right)^2 \right]} \quad (A1)$$

The ideal average kinetic energy is related to the actual kinetic energy by

$$\left(\frac{V_{av}}{a_{cr}}\right)_{id}^2 = \left(\frac{V_{av}}{a_{cr}}\right)^2 + \lambda \left(\frac{V_{av}}{a_{cr}}\right)^2 \quad (A2)$$

then

$$\lambda = \frac{\left(\frac{V_{av}}{a_{cr}}\right)_{id}^2}{\left(\frac{V_{av}}{a_{cr}}\right)^2} - 1 \quad (A3)$$

The total-pressure loss can be expressed as a function of  $V_{av}/a_{cr}$  and  $\lambda$  by using the isentropic relation

$$\frac{p}{P} = \left[ 1 - \frac{\gamma - 1}{\gamma + 1} \left(\frac{V_{av}}{a_{cr}}\right)^2 \right]^{\frac{\gamma}{\gamma - 1}} \quad (A4)$$

Combination of equations (A3) and (A4) gives

$$\frac{P_e}{P_{in}} = \left[ \frac{1 - \frac{\gamma - 1}{\gamma + 1} \left(\frac{V_{av}}{a_{cr}}\right)^2 \lambda}{1 - \frac{\gamma - 1}{\gamma + 1} \left(\frac{V_{av}}{a_{cr}}\right)^2} \right]^{\frac{\gamma}{\gamma - 1}} \quad (A5)$$

Equation (A5) can be written for a given blade row, that is, the inlet stator, as

$$\frac{P_2}{P_1} = \left[ 1 - \frac{\frac{\gamma - 1}{\gamma + 1} \left( \frac{V_{av}}{a_{cr}} \right)^2 \lambda}{1 - \frac{\gamma - 1}{\gamma + 1} \left( \frac{V_{av}}{a_{cr}} \right)^2} \right]^{\frac{\gamma}{\gamma - 1}} \quad (A6)$$

A solution for the loss parameter  $\lambda$  gives

$$\lambda = \frac{1 - \frac{\gamma - 1}{\gamma + 1} \left( \frac{V_{av}}{a_{cr}} \right)^2}{\frac{\gamma - 1}{\gamma + 1} \left( \frac{V_{av}}{a_{cr}} \right)^2} \left[ 1 - \left( \frac{P_2}{P_1} \right)^{\frac{\gamma - 1}{\gamma}} \right] \quad (A7)$$

Thus  $\lambda$  may be expressed for any blade row by using the average of the relative inlet and exit critical velocity ratios and a total-pressure loss relative to the blade at the operating point where these velocities exist.

A relation is desired between the loss parameter  $\lambda$  and the Reynolds number. In order to do this the loss parameter is first determined as a function of the boundary-layer momentum thickness  $\theta^*$ , so that Prandtl 1/5th-power law as expressed in equation (1) may be used.

The total-pressure loss used in calculating the loss parameter  $\lambda$  for a blade row is expressed as a function of the design flow conditions and the displacement thickness  $\delta^*$  in the plane of the trailing edge and at the blade exit by equation (C22) of reference 15:

$$\frac{P_m}{P_{in}} = \frac{\left( \frac{\rho V}{\rho_T V_{cr}} \right)_{fs,n} \cos \alpha_n \left( 1 - \frac{\delta^* + t}{s \cos \alpha_e} \right)}{\left( \frac{\rho V_z}{\rho_T V_{cr}} \right)_m} \quad (A8)$$

The momentum thickness is proportional to the viscous loss and is related to the displacement thickness by the form factor  $H$  as

$$H = \frac{\delta^*}{\theta^*} \quad (A9)$$

where  $H$  is a function of the free-stream critical velocity ratio and the boundary-layer velocity profile as expressed by equation (B12) of reference 15. This relation accounts for compressibility effects at the higher critical velocity ratios. A chart of  $H$  as a function of the critical velocity ratio  $V/a_{cr}$  for a  $1/7$ th-power boundary-layer velocity profile was used in the present calculation.

In order to obtain the loss parameter  $\lambda$  at a given Reynolds number, the Prandtl relation of equation (1) is written as

$$\frac{\theta^*}{\theta_{ref}^*} = \left( \frac{Re_{ref}}{Re} \right)^{1/5} \quad (A10)$$

#### Calculation of Loss Parameter at the Reference Reynolds Number

Use of either experimentally determined or assumed values of velocities and total-pressure losses through the turbine enables a value of  $\lambda$  for each blade row to be calculated for the design condition by use of equation (A7). This value of  $\lambda$  for each blade row is then held constant in the calculation of the predicted over-all turbine performance at the reference Reynolds number.

Variation of  $\lambda$  with Reynolds number. - In order to obtain the loss parameter  $\lambda$  at any given Reynolds number other than the reference value, the following procedure is used.

(1) The momentum thickness  $\theta_{ref}^*$  at the reference Reynolds number is calculated using equations (A9) and (A8) as follows: The form factor  $H$  is determined from the known velocities at the turbine design point with an assumed value of  $\theta_{ref}^*$ ;  $\delta^*$  can be obtained from equation (A9). The parameter  $\delta^*$  is then used in equation (A8) to obtain the total-pressure loss for a blade row. The pressure loss is calculated using successive values of  $\theta_{ref}^*$  in an iterative process until agreement is obtained between calculated and experimental values.

(2) The momentum thickness  $\theta^*$  for the desired Reynolds number is calculated from equation (A10).

(3) With the momentum thickness  $\theta^*$  corresponding to the desired Reynolds number, the total-pressure loss for each blade row is calculated using equations (A8) and (A9). The velocities used in obtaining the value of parameter  $H$  and those used in equation (A9) were the design values at the reference conditions.

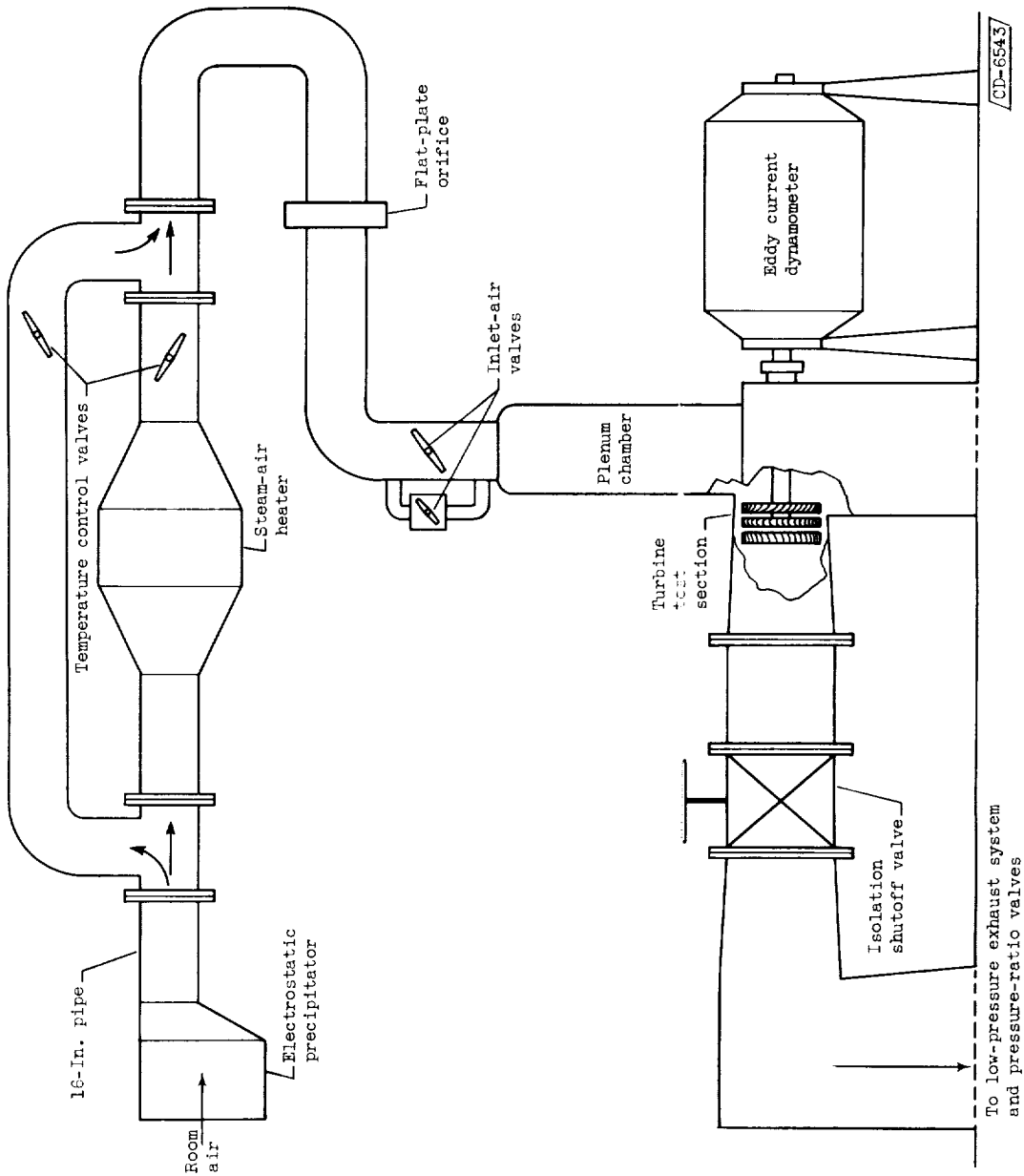
(4) The value of the loss parameter  $\lambda$  for each blade row corresponding to the desired Reynolds number is calculated using equation (A7). The calculated value of the loss parameter  $\lambda$  for each blade row is then used in the theoretical performance prediction method.

#### REFERENCES

1. Kaufman, Harold R.: Some Reynolds Number Phenomena in a Turbojet Compressor. NACA RM E57D01, 1957.
2. Walker, Curtis L., Huntley, S. C., and Braithwaite, W. M.: Component and Over-All Performance Evaluation of an Axial-Flow Turbojet Engine over a Range of Engine-Inlet Reynolds Numbers. NACA RM E52B08, 1952.
3. Geye, Richard P., and Lucas, James G.: Investigation of Effects of Reynolds Number on Over-All Performance of an Eight-Stage Axial-Flow Research Compressor with Two Transonic Inlet Stages. NACA RM E56L11a, 1957.
4. Neustein, Joseph: Experiments at Low Reynolds Numbers. Pt. II. - Axial Flow Turbomachine. Rep. No. 6, Hydrodynamics and Mech. Eng. Lab., C.I.T., Mar. 1957. (Navy Contract Nonr-220(23).)
5. Carter, A. D. S., Moss, C. E., Green, G. R., and Annear, G. G.: The Effect of Reynolds Number on the Performance of a Single Stage Compressor. Rep. No. R.204, British NGTE, May 1957.
6. Schum, Harold J.: Performance Evaluation of Reduced-Chord Rotor Blading as Applied to J73 Two-Stage Turbine. V - Effect of Inlet Pressure on Over-All Performance at Design Speed and Inlet Temperature of 700° R. NACA RM E53L16b, 1957.
7. Whitney, Warren J., and Wintucky, William F.: Experimental Investigation of a 7-Inch-Tip-Diameter Transonic Turbine. NACA RM E57J29, 1958.
8. Gabriel, David S., Carman, L. Robert, and Frautwein, Elmer E.: The Effect of Inlet Pressure and Temperature on the Efficiency of a Single-Stage Impulse Turbine Having an 11.0-Inch Pitch-Line Diameter Wheel. NACA WR E-216, 1945. (Supersedes NACA ACR E5E19.)
9. Plohr, Henry W., Holeski, Donald E., and Forrette, Robert E.: Design and Experimental Investigation of a Single-Stage Turbine with a Downstream Stator. NACA RM E56K10, 1957.

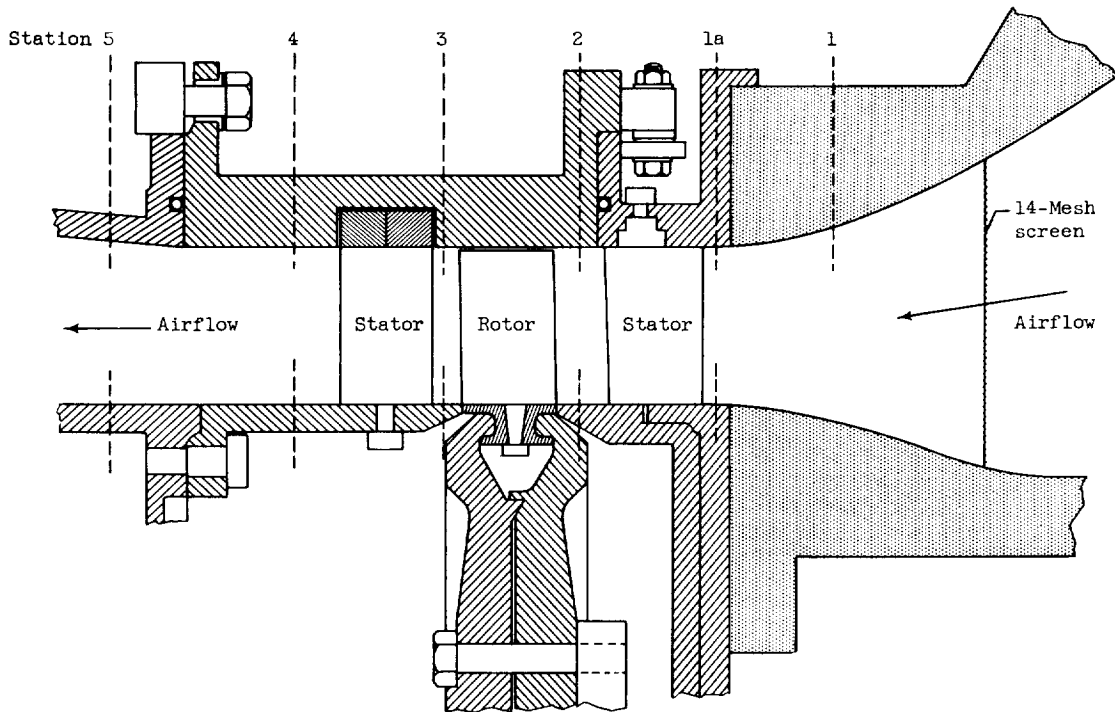


10. Mickelsen, William R.: An Experimental Comparison of the Lagrangian and Eulerian Correlation Coefficients in Homogeneous Isotropic Turbulence. NACA TN 3570, 1955.
11. Dryden, Hugh L., and Abbott, Ira H.: The Design of Low-Turbulence Wind Tunnels. NACA Rep. 940, 1949. (Supersedes NACA TN 1755.)
12. Kochendorfer, Fred D., and Nettles, J. Cary: An Analytical Method of Estimating Turbine Performance. NACA Rep. 930, 1949. (Supersedes NACA RM E8I16.)
13. Stewart, Warner L., and Evans, David G.: Analytical Study of Losses at Off-Design Conditions for a Fixed-Geometry Turbine. NACA RM E53K06, 1954.
14. Schlichting, Hermann: Boundary Layer Theory. McGraw-Hill Book Co., Inc., 1955, p. 432.
15. Stewart, Warner L.: Analysis of Two-Dimensional Compressible-Flow Loss Characteristics Downstream of Turbomachine Blade Rows in Terms of Basic Boundary-Layer Characteristics. NACA TN 3515, 1955.

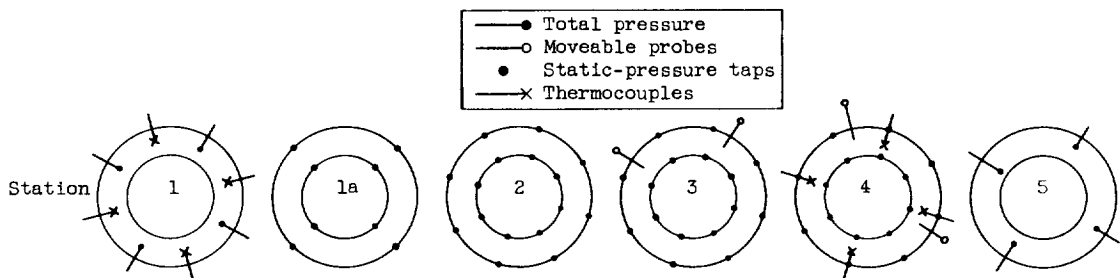


(a) Sketch showing airflow path.

Figure 1. - Schematic sketch of experimental equipment.



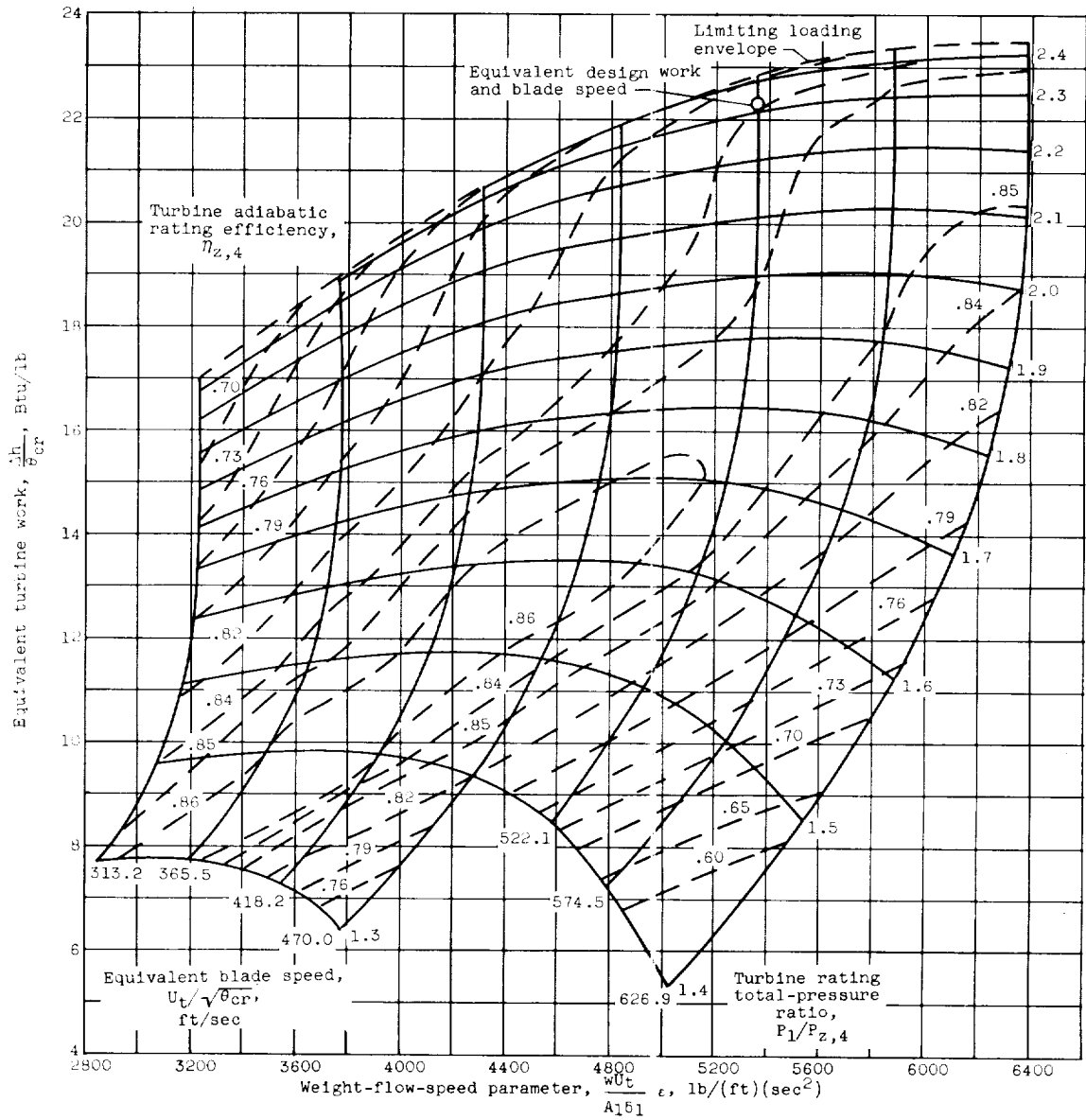
Cross section of turbine showing measuring stations.



(b) Location of instrumentation at each axial station.

CD-6542/

Figure 1. - Concluded. Schematic sketch of experimental equipment.



(a) Reynolds number, 182,500.

Figure 2. - Experimental turbine performance map.

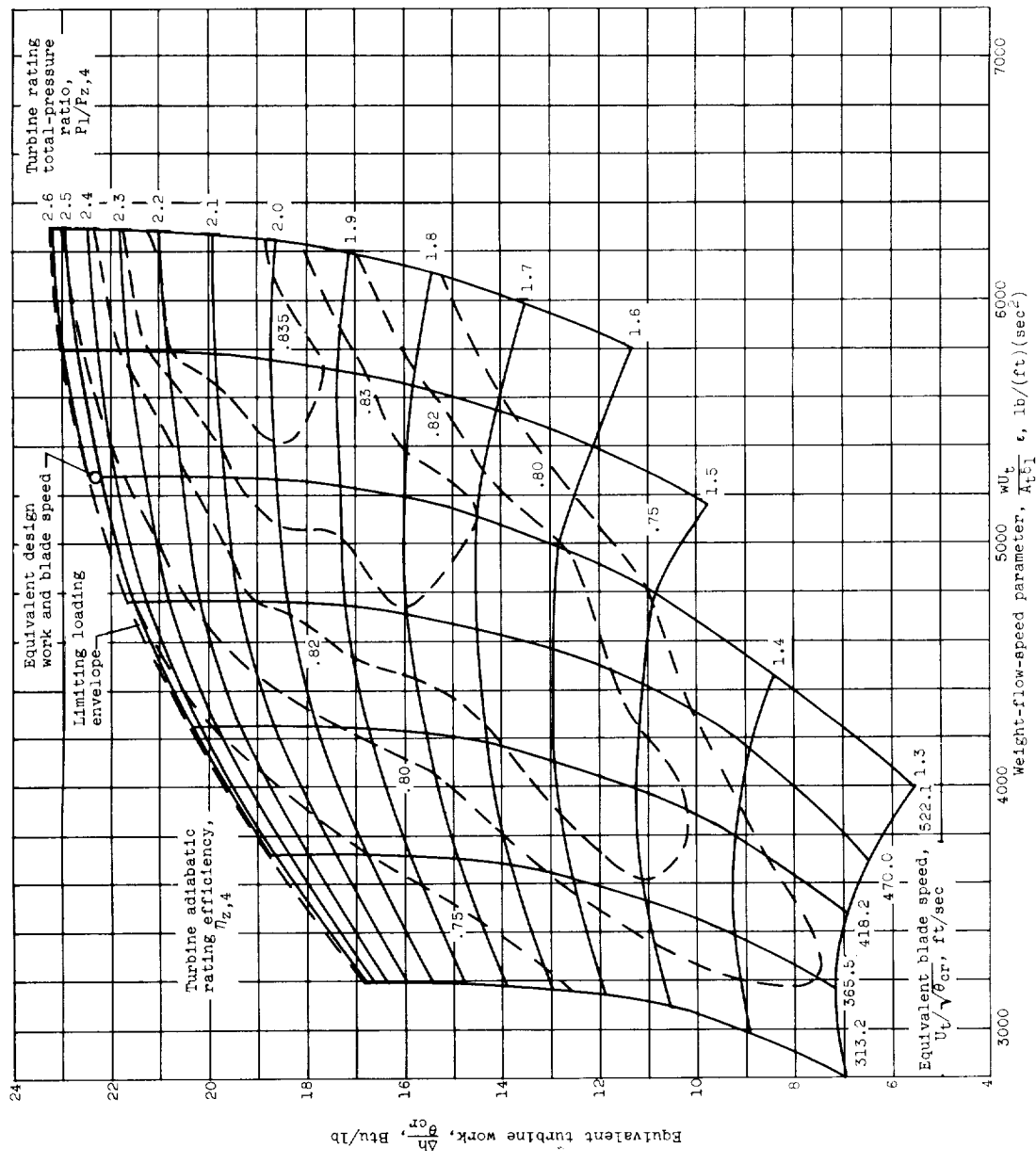
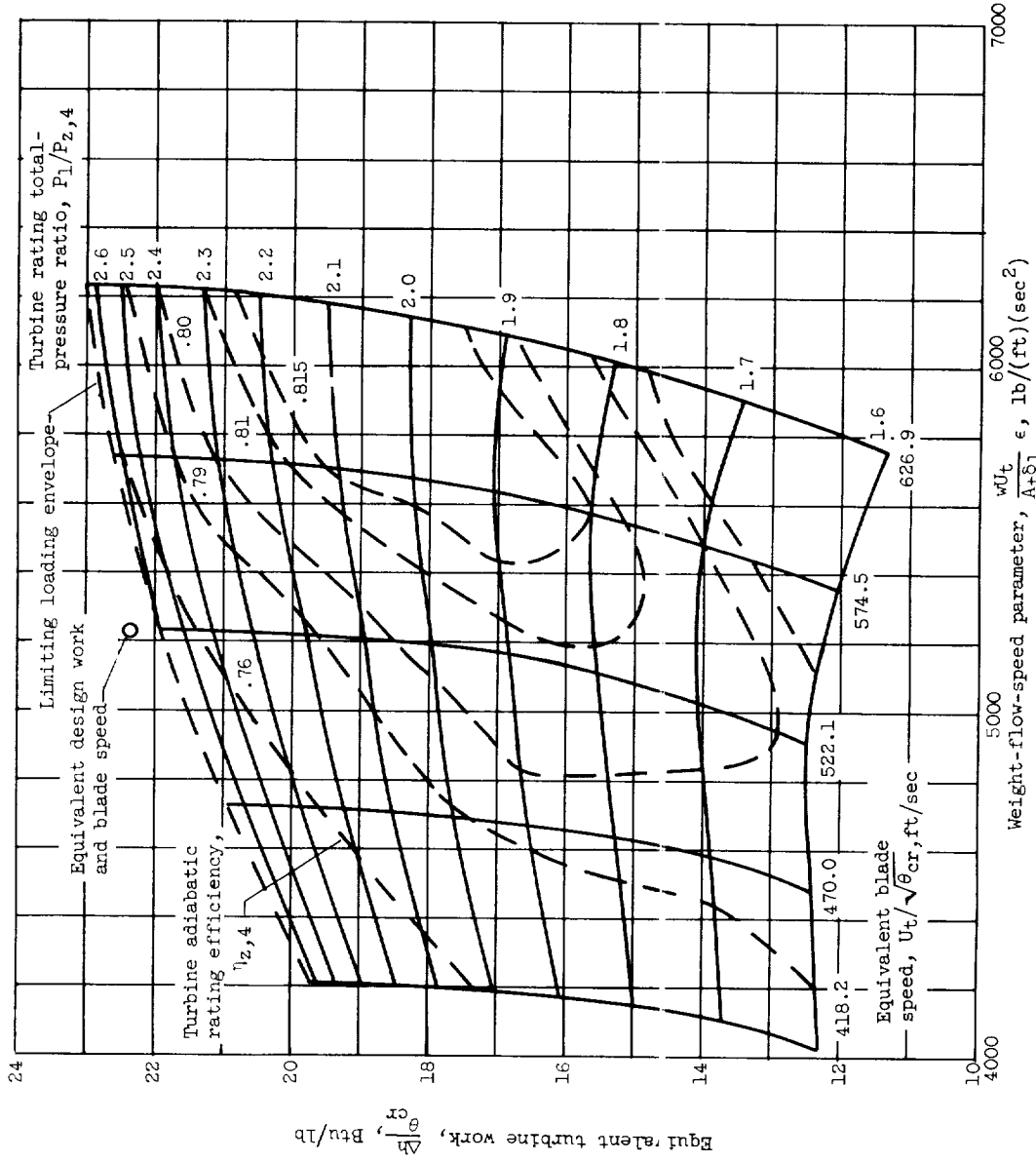
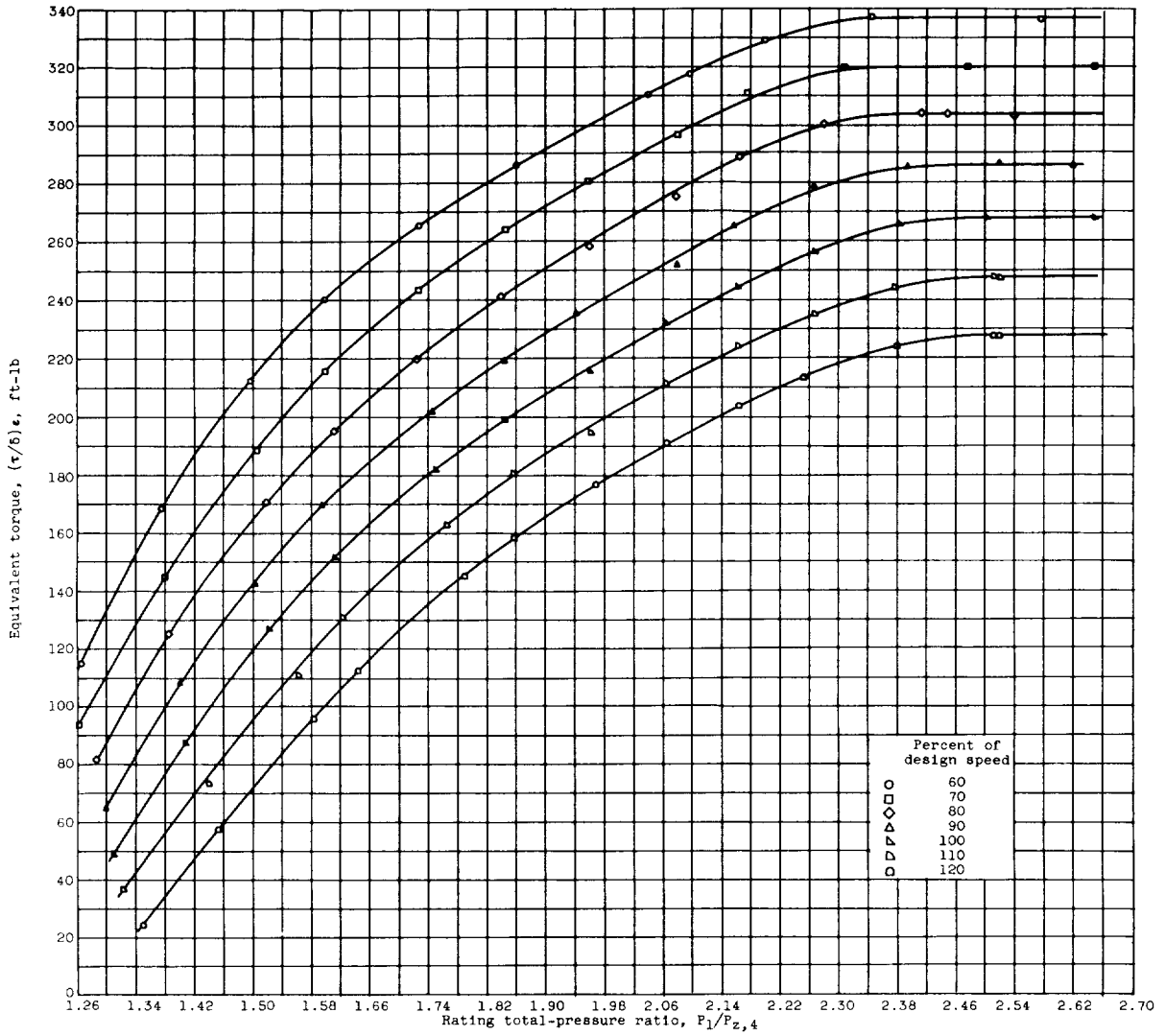


Figure 2. - Continued. Experimental turbine performance map.



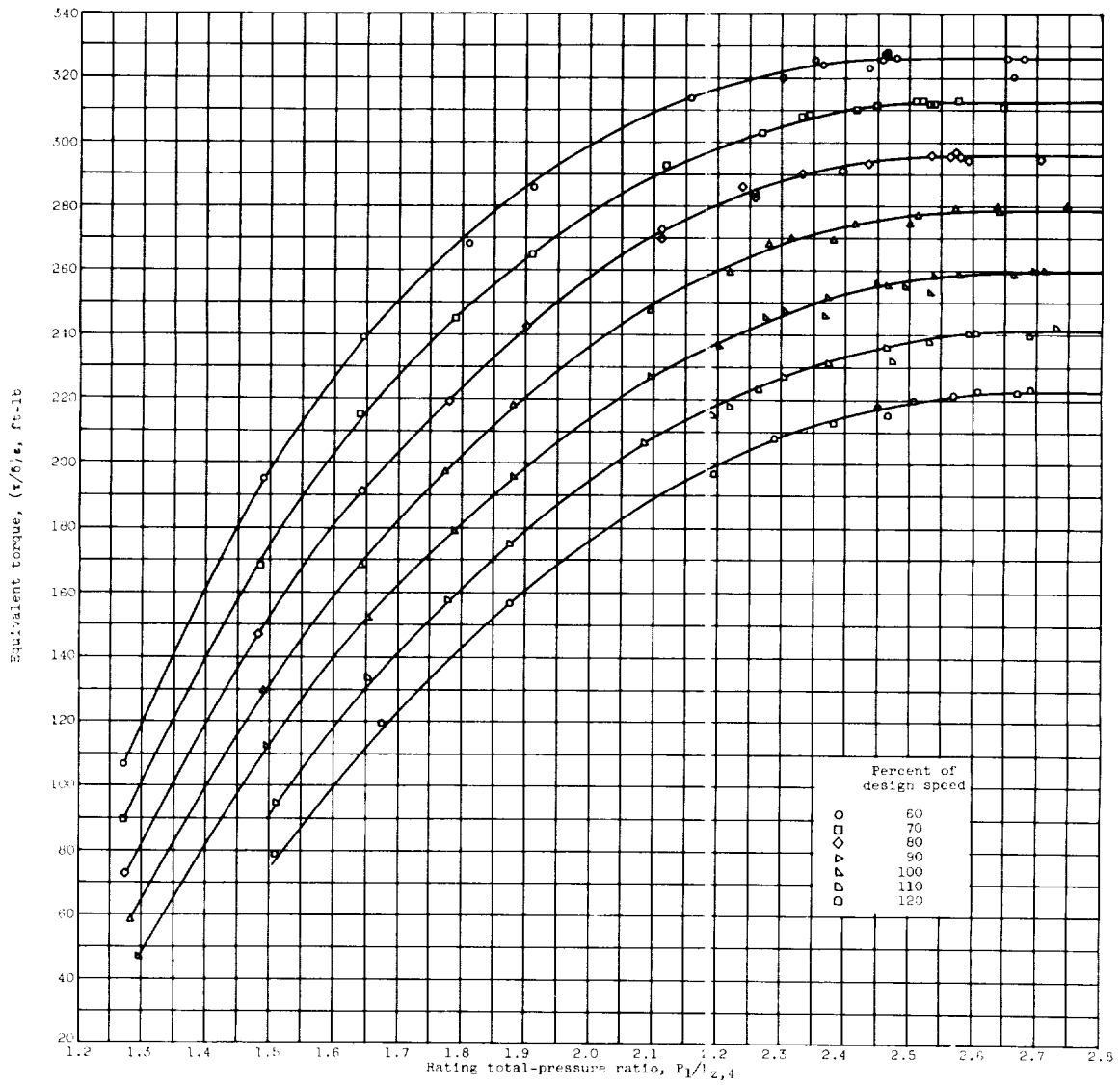
(c) Reynolds number, 23,000.  
 Figure 2. - Concluded. Experimental turbine performance map.

E-185



(a) Reynolds number, 182,500.

Figure 3. - Variation of equivalent torque with rating total-pressure ratio for values of constant equivalent blade speed.



(b) Reynolds number, 39,600.

Figure 3. - Continued. Variation of equivalent torque with rating total-pressure ratio for values of constant equivalent blade speed.



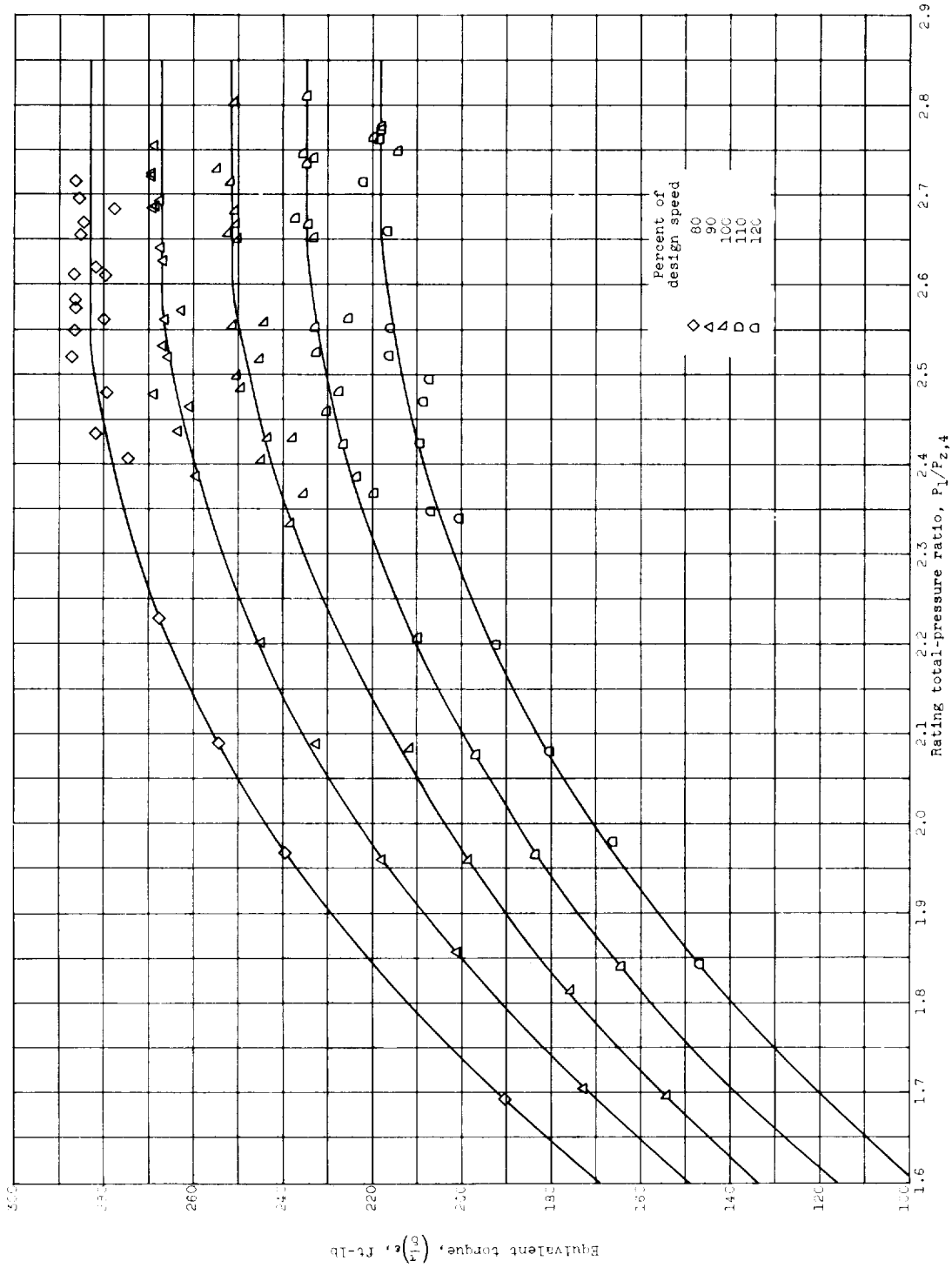
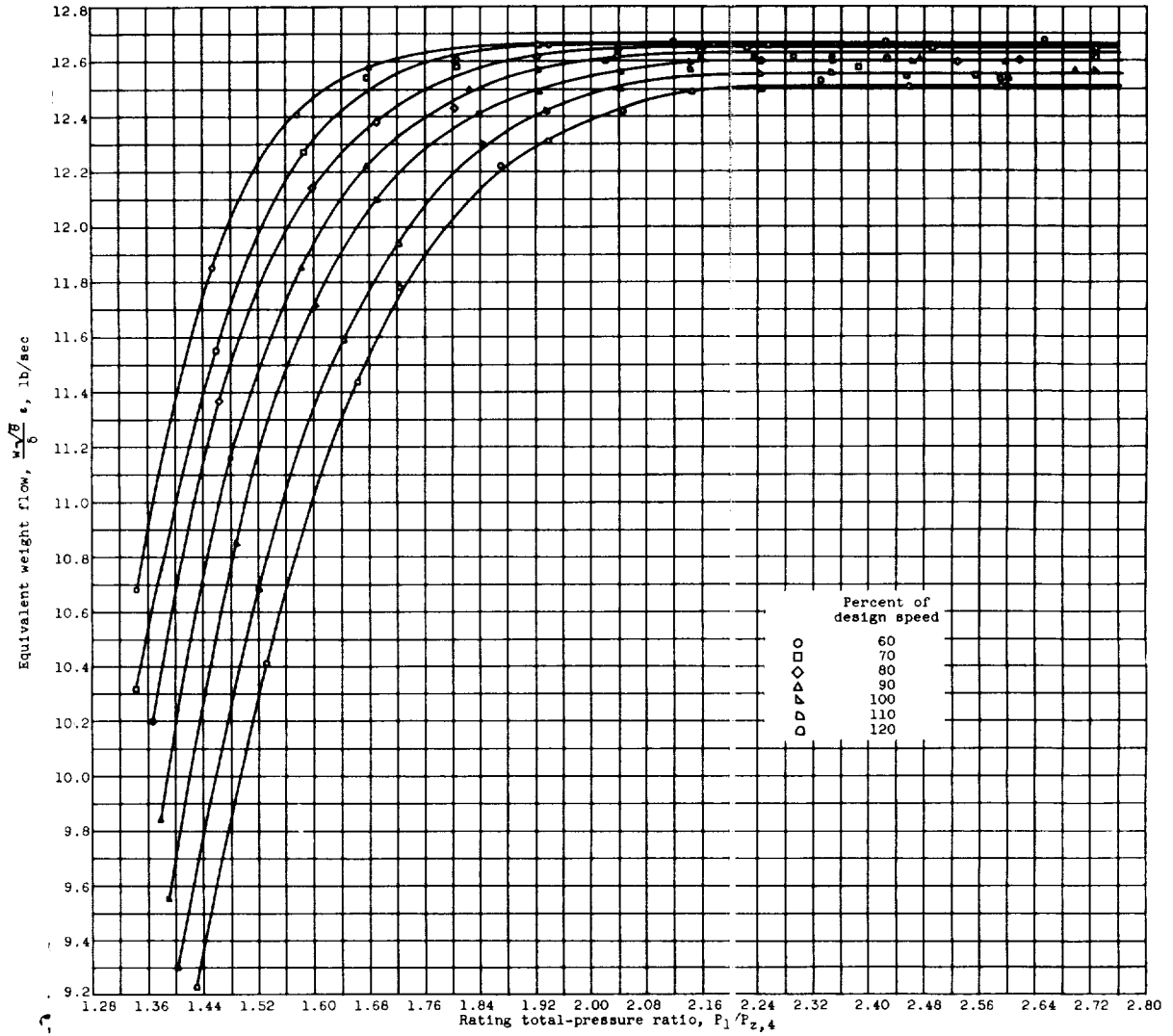
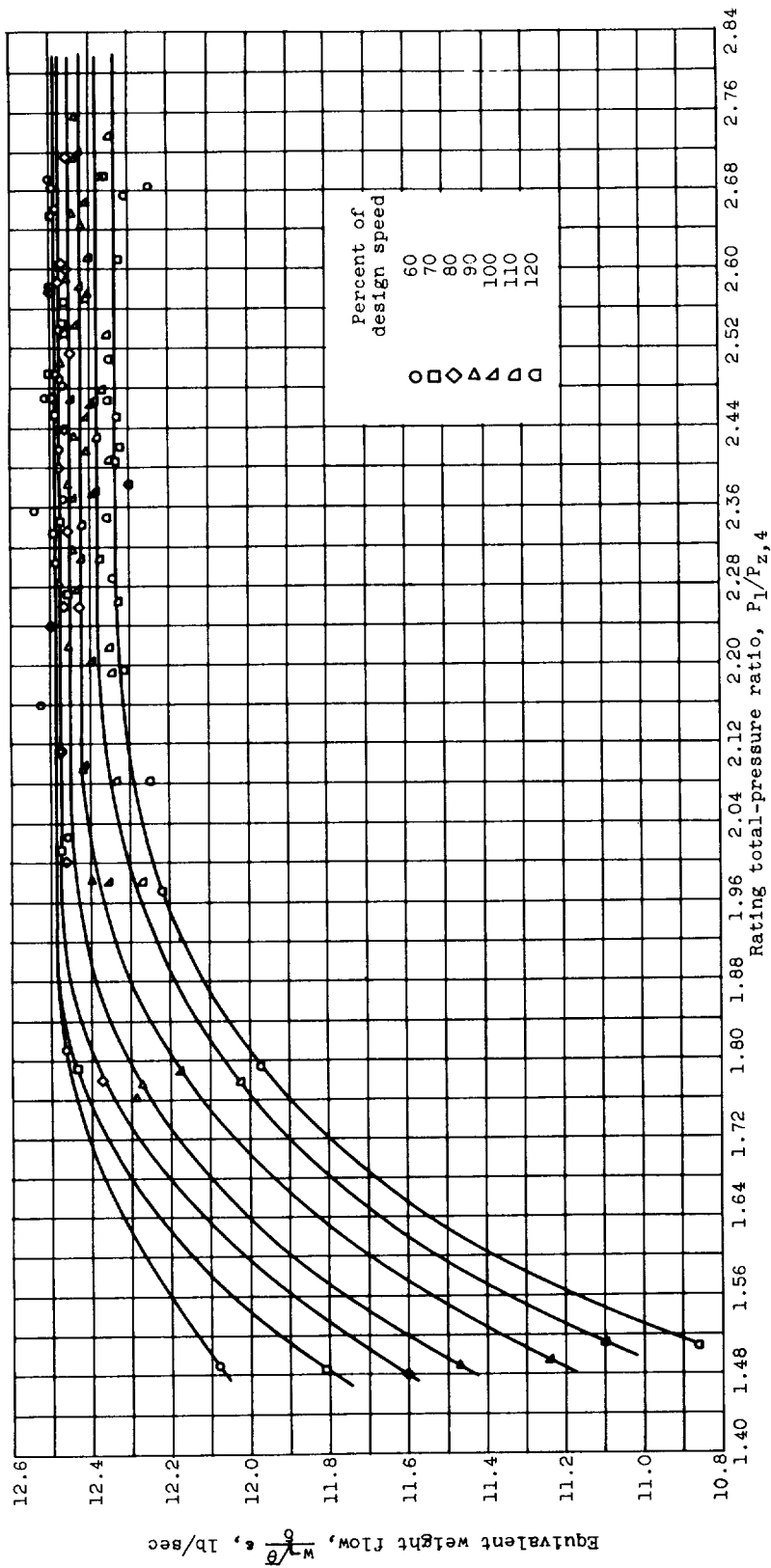


Figure 3. - Concluded. Variation of equivalent torque with rating total-pressure ratio for values of equivalent blade speed.

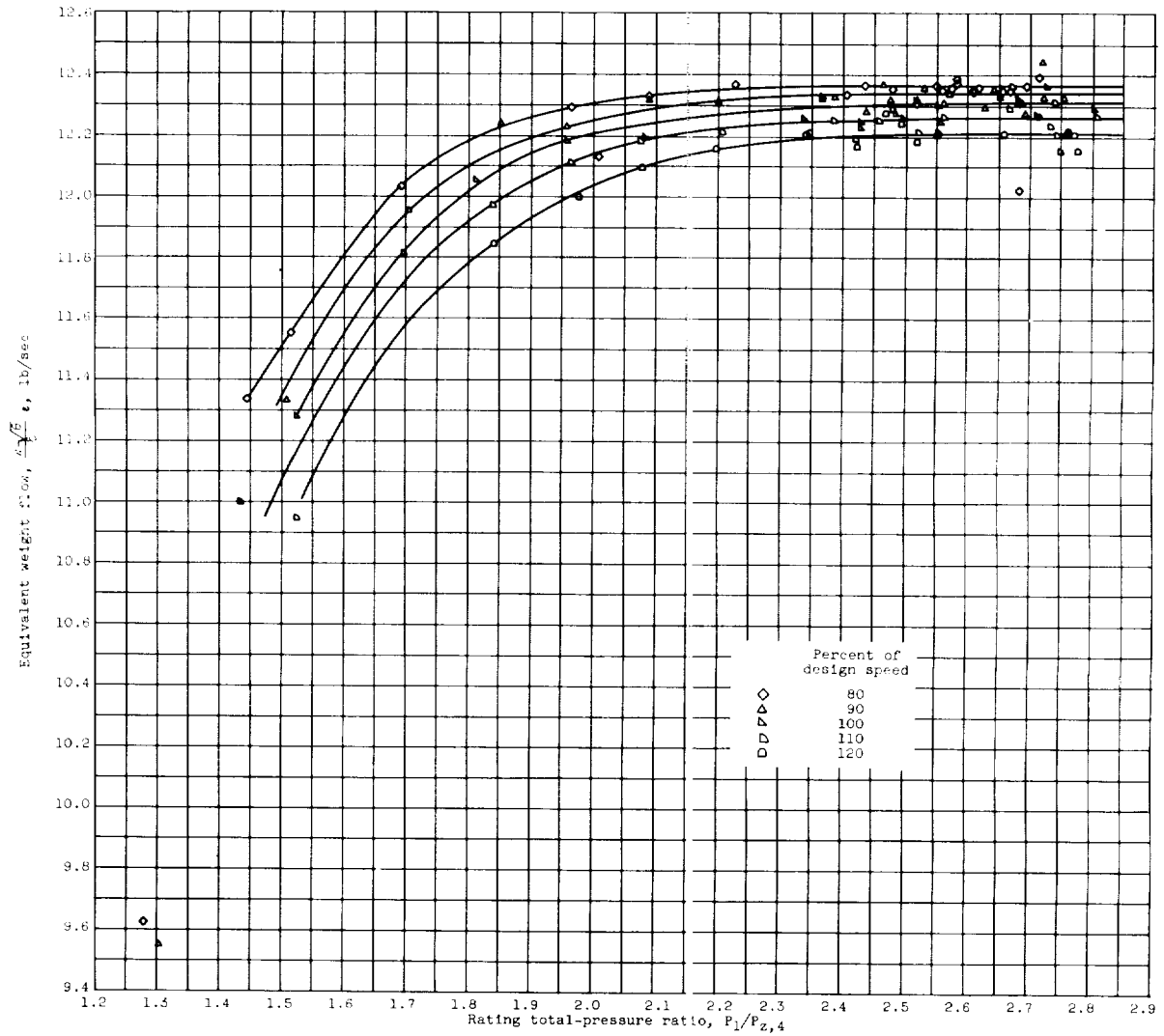


(a) Reynolds number, 182,500.

Figure 4. - Variation of equivalent weight flow with rating total-pressure ratio for values of constant equivalent blade speed.

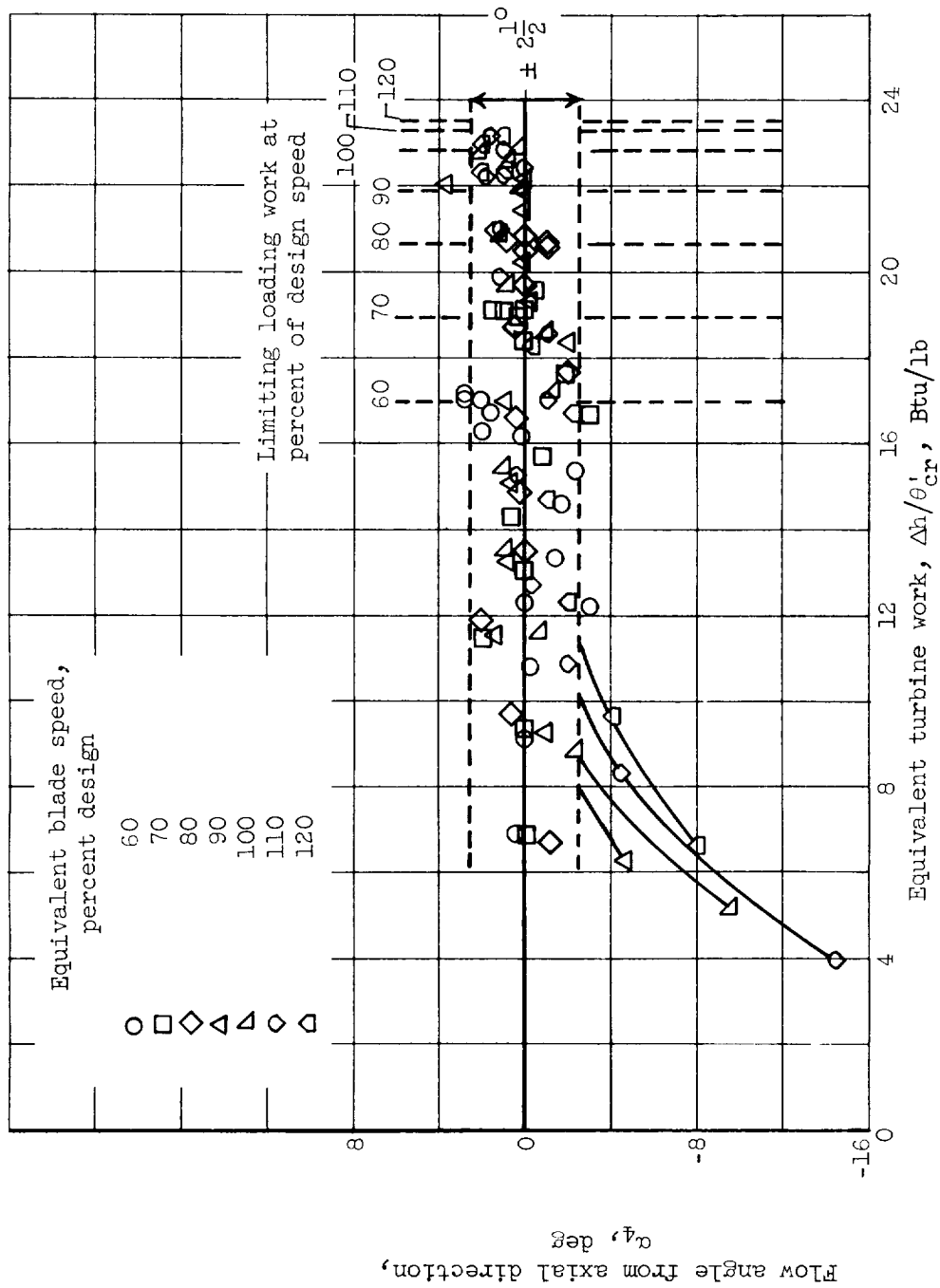


(b) Reynolds number, 39,600  
 Figure 4. - Continued. Variation of equivalent weight flow with rating total-pressure ratio for values of equivalent blade speed.



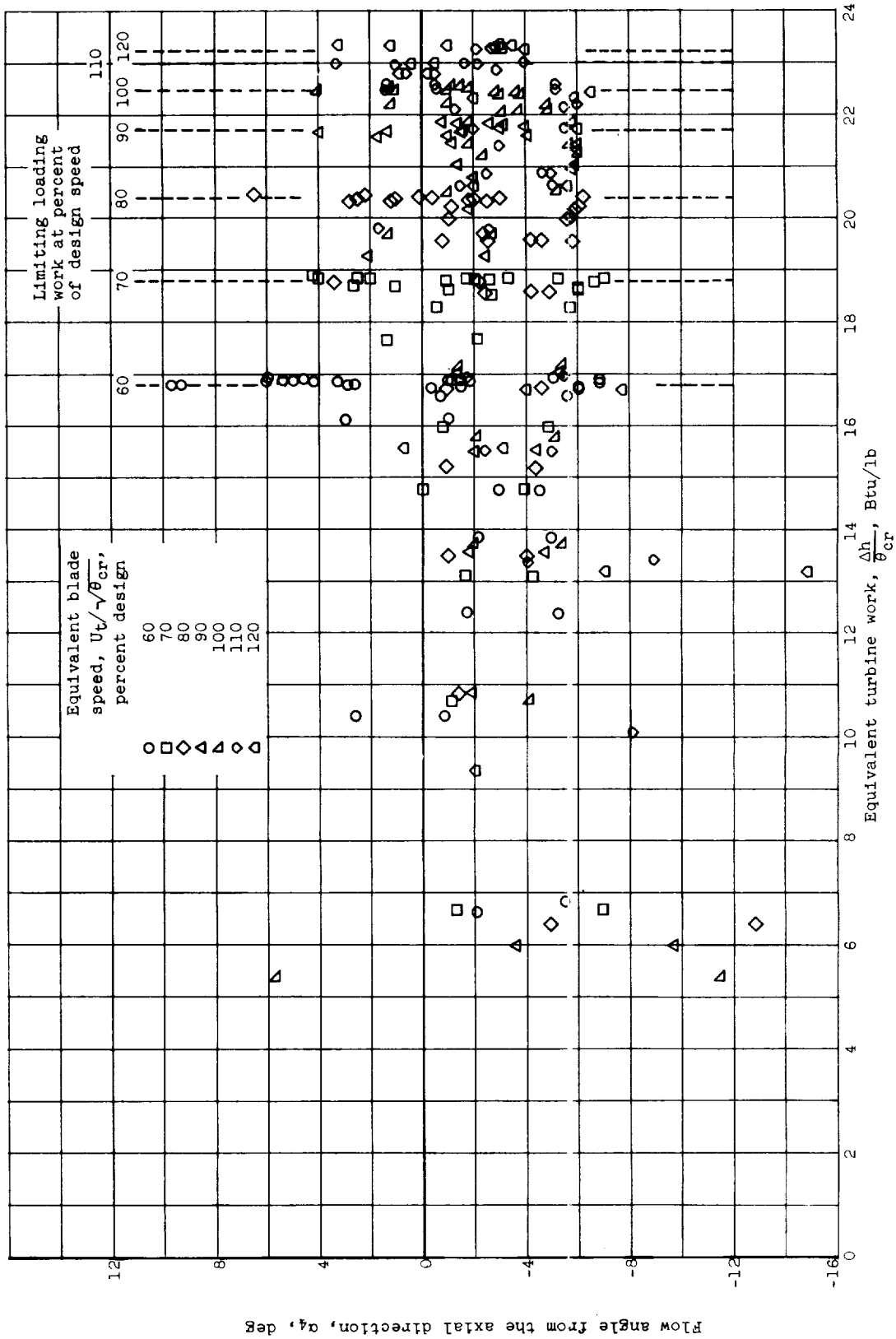
(c) Reynolds number, 23,000.

Figure 4. - Concluded. Variation of equivalent weight flow with rating total-pressure ratio for values of equivalent blade speed.



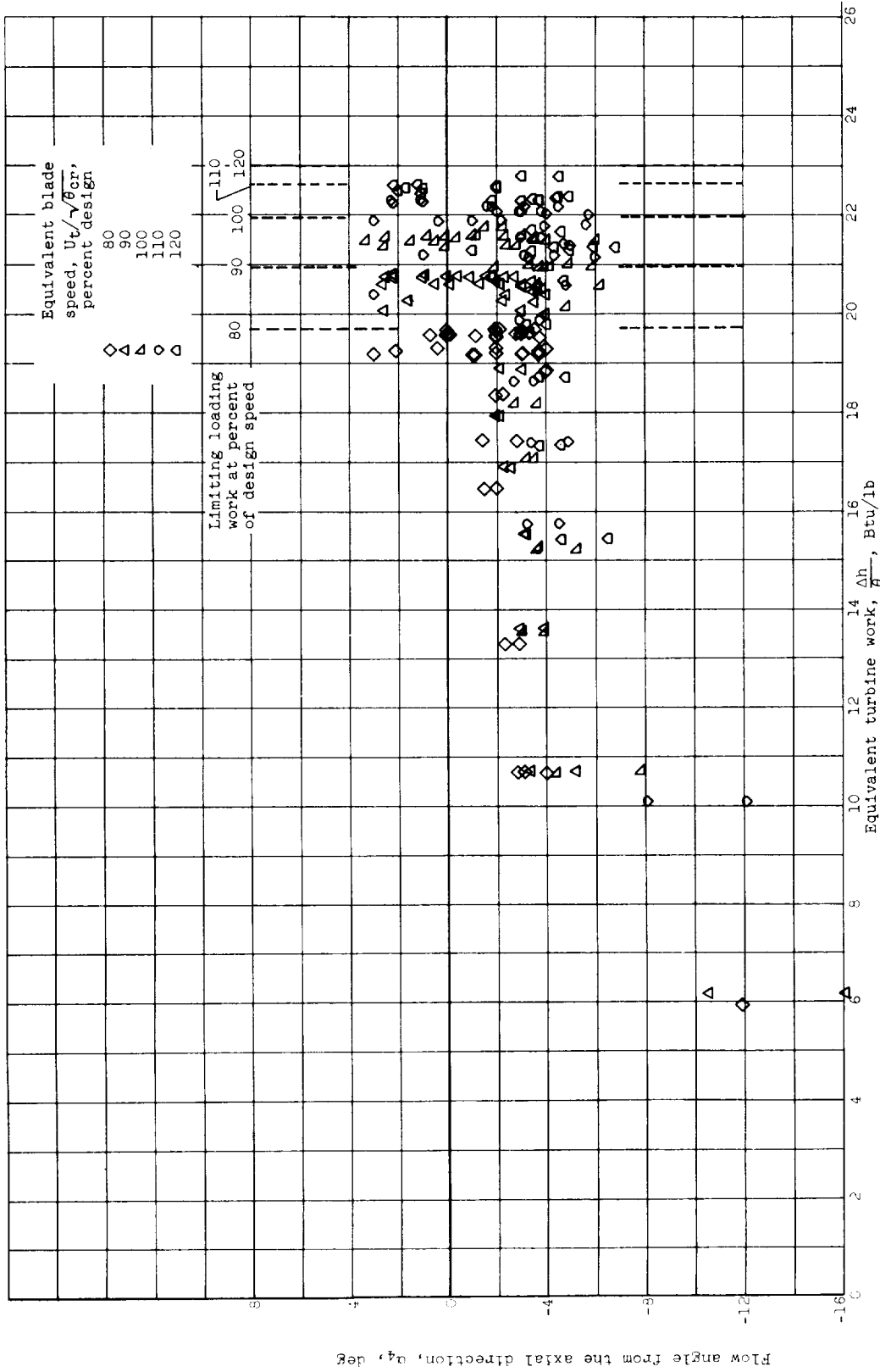
(a) Reynolds number, 182,500.

Figure 5. - Absolute flow angle at exit of downstream stator as a function of equivalent work and speed.



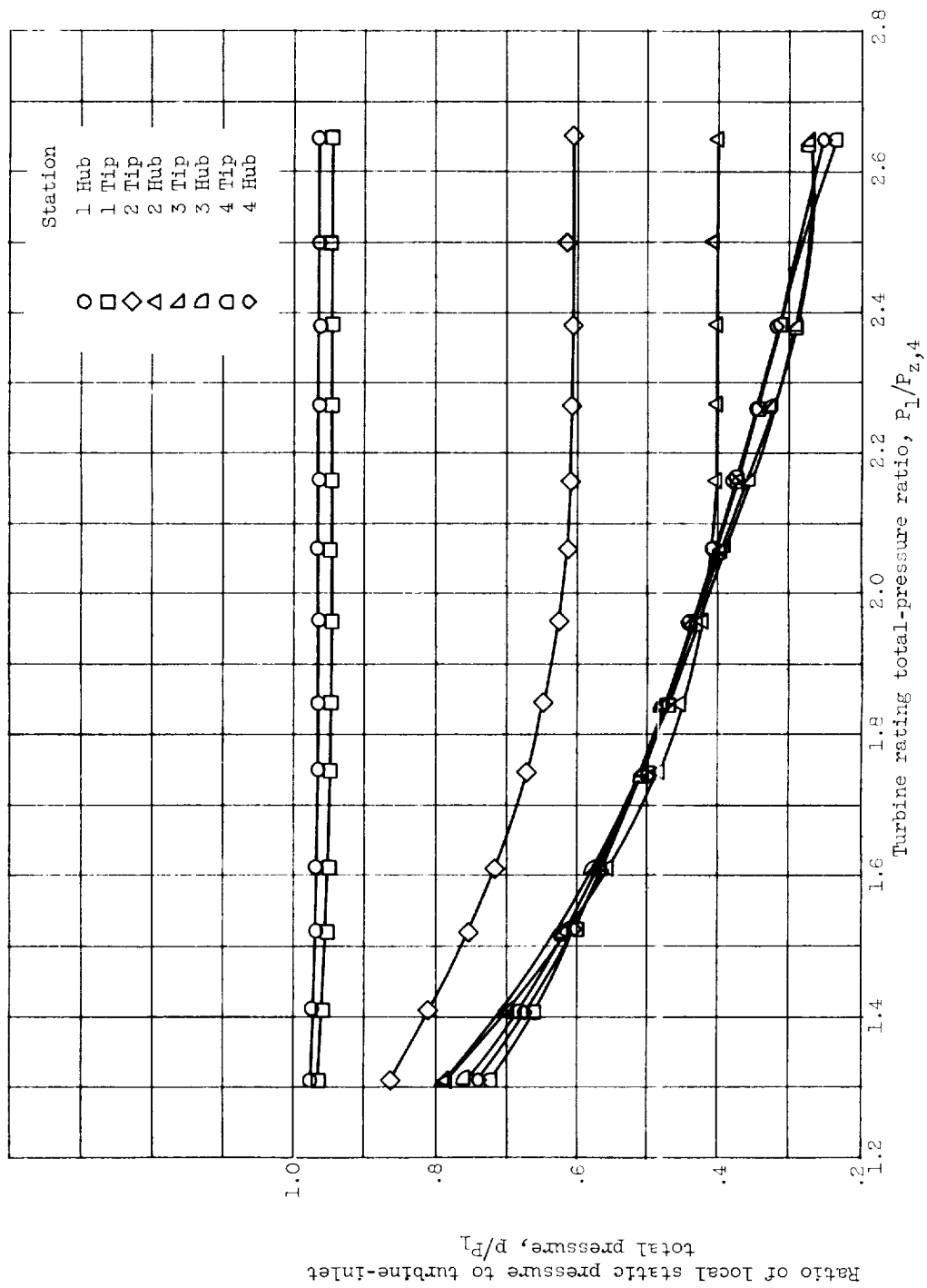
(b) Reynolds number, 39,600.

Figure 5. - Continued. Absolute flow angle at exit of downstream stator as a function of equivalent work and speed.



(c) Reynolds number, 23,000.

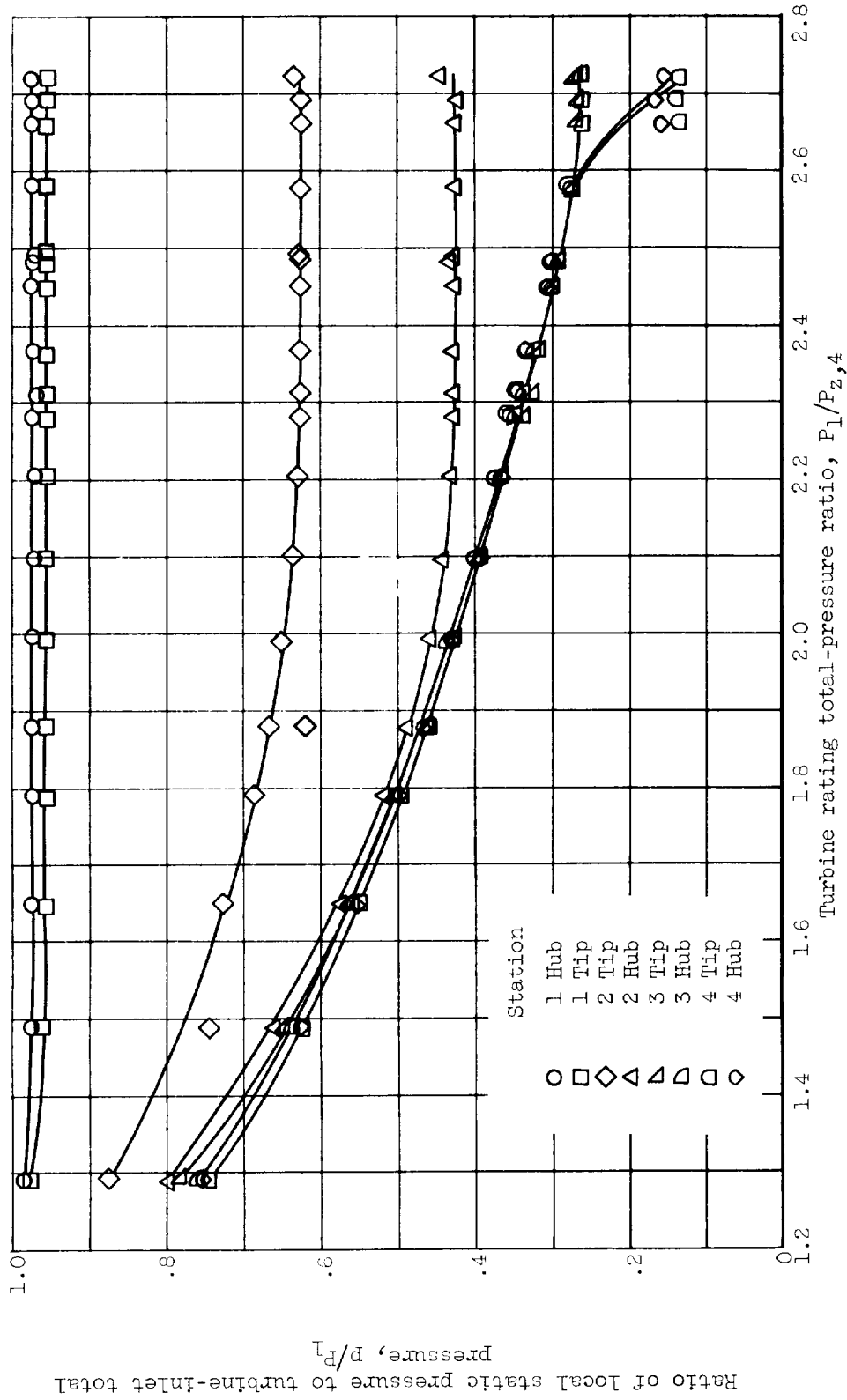
Figure 5. - Concluded. Absolute flow angle at exit of downstream stator as a function of equivalent work and speed.



(a) Reynolds number, 182,500.

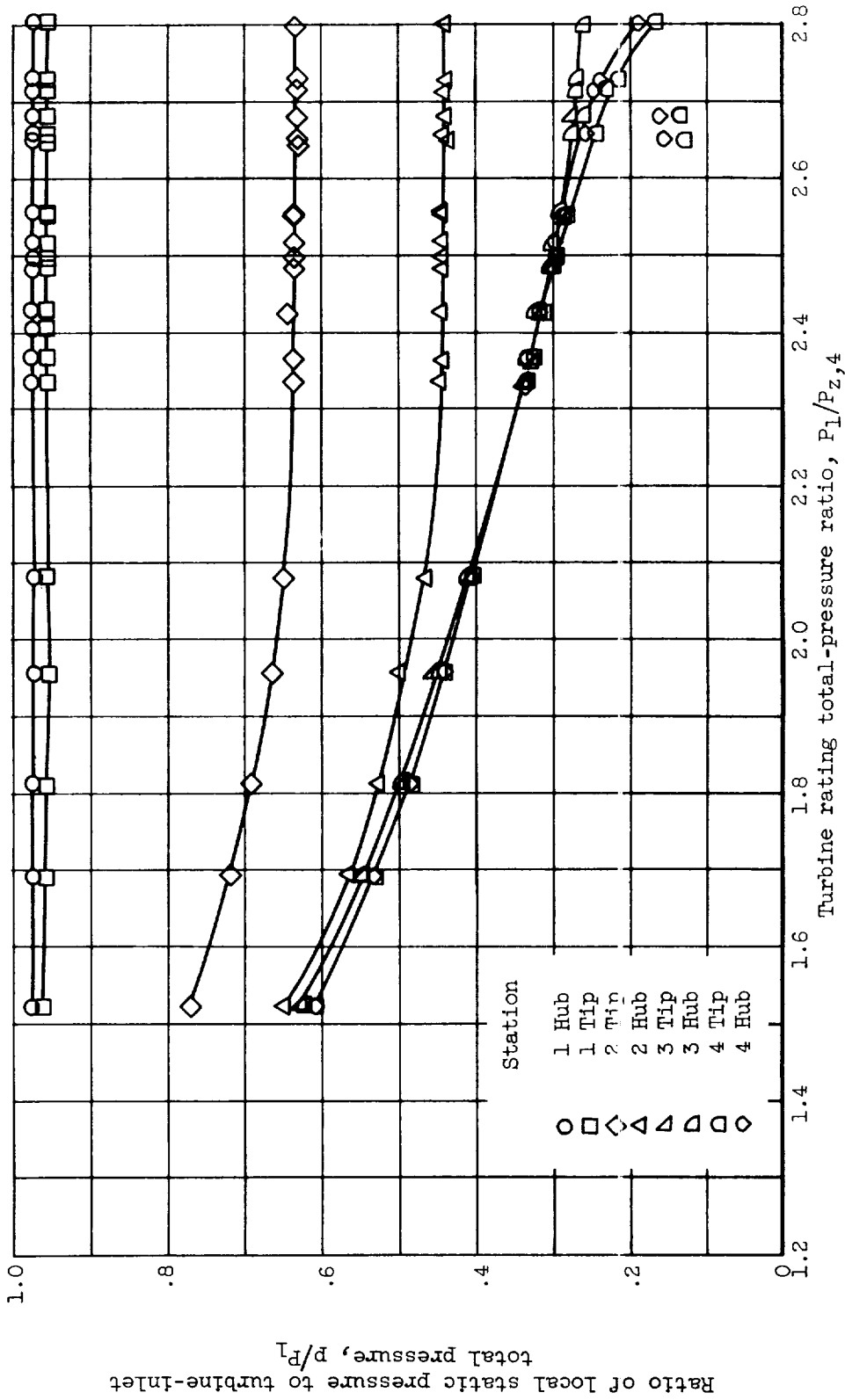
Figure 6. - Variation of static pressure with turbine rating total-pressure ratio at four axial measuring stations and 100-percent design speed.





(b) Reynolds number, 39,600.

Figure 6. - Continued. Variation of static pressure with turbine rating total-pressure ratio at four axial measuring stations and 100-percent design speed.



(c) Reynolds number, 23,000.

Figure 6. - Concluded. Variation of static pressure with turbine rating total-pressure ratio at four axial measuring stations and 100-percent design speed.

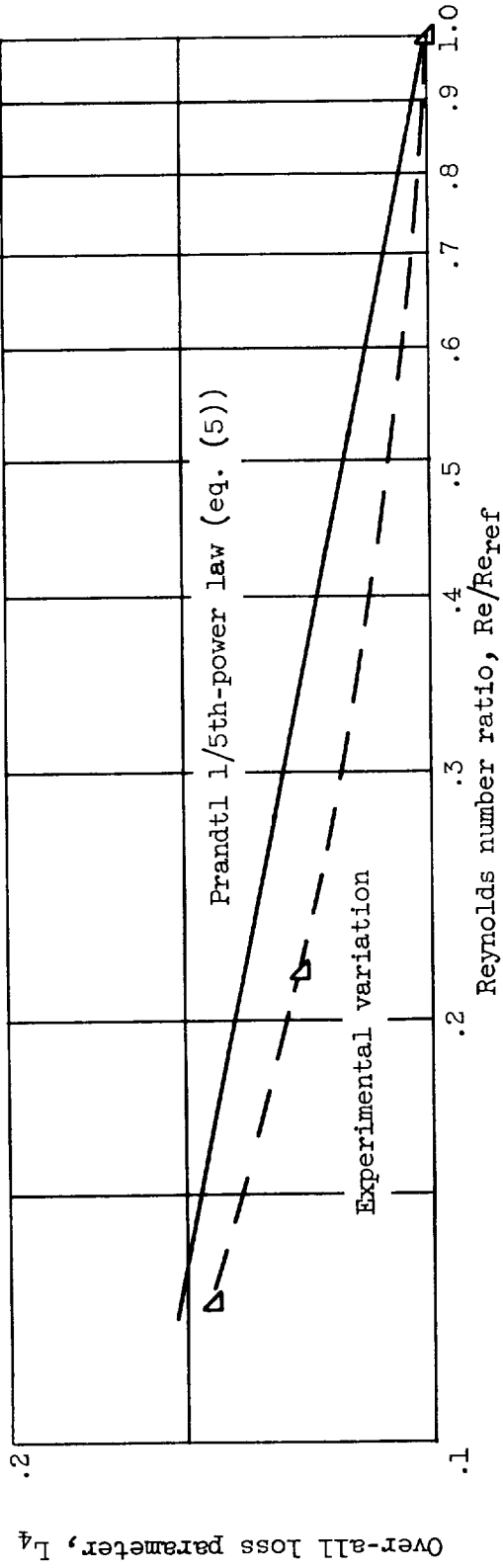


Figure 7. - Variation of over-all turbine loss parameter with Reynolds number.

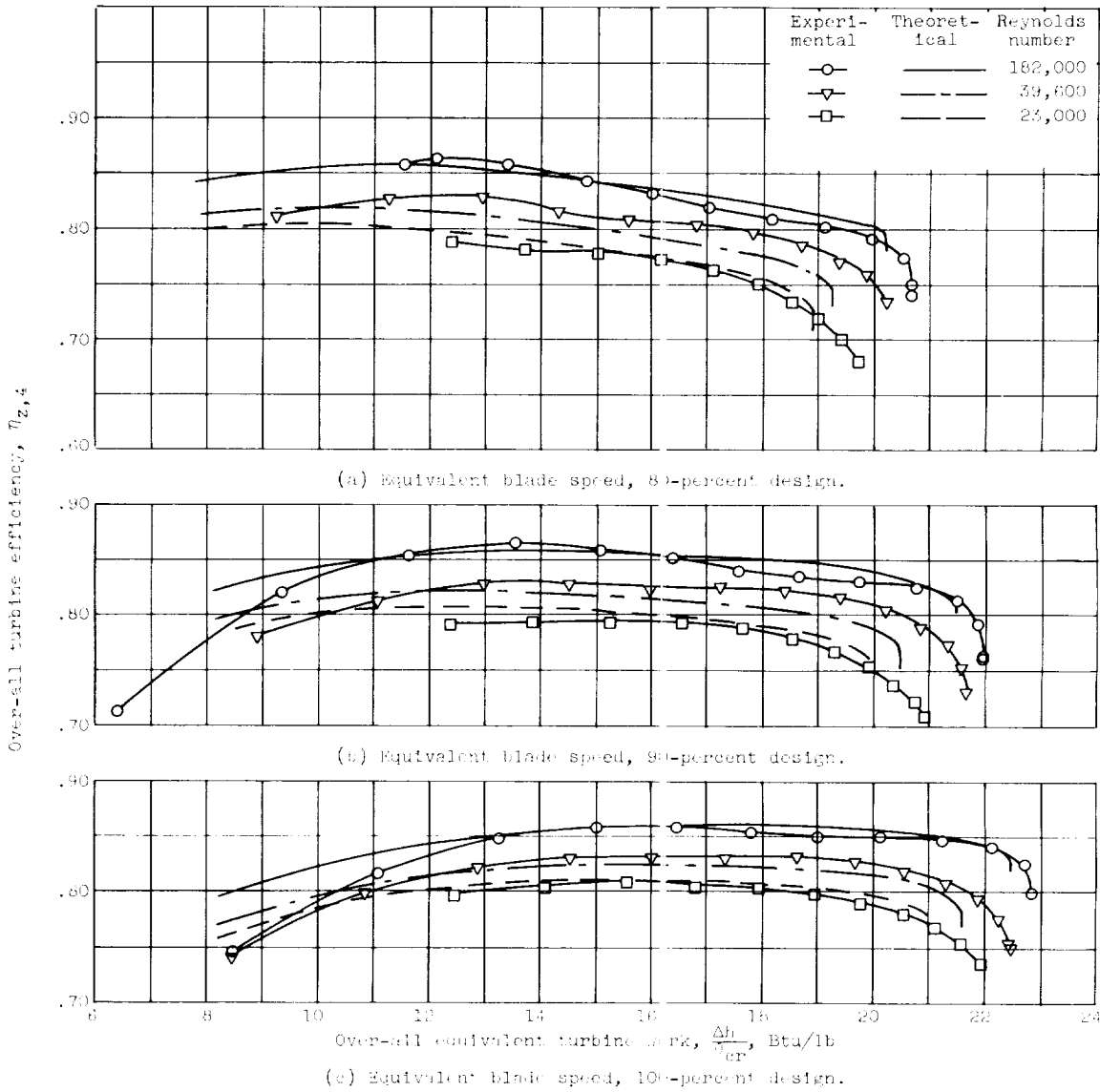


Figure 8. - Experimental and theoretical over-all efficiency as a function of equivalent turbine work and Reynolds number.

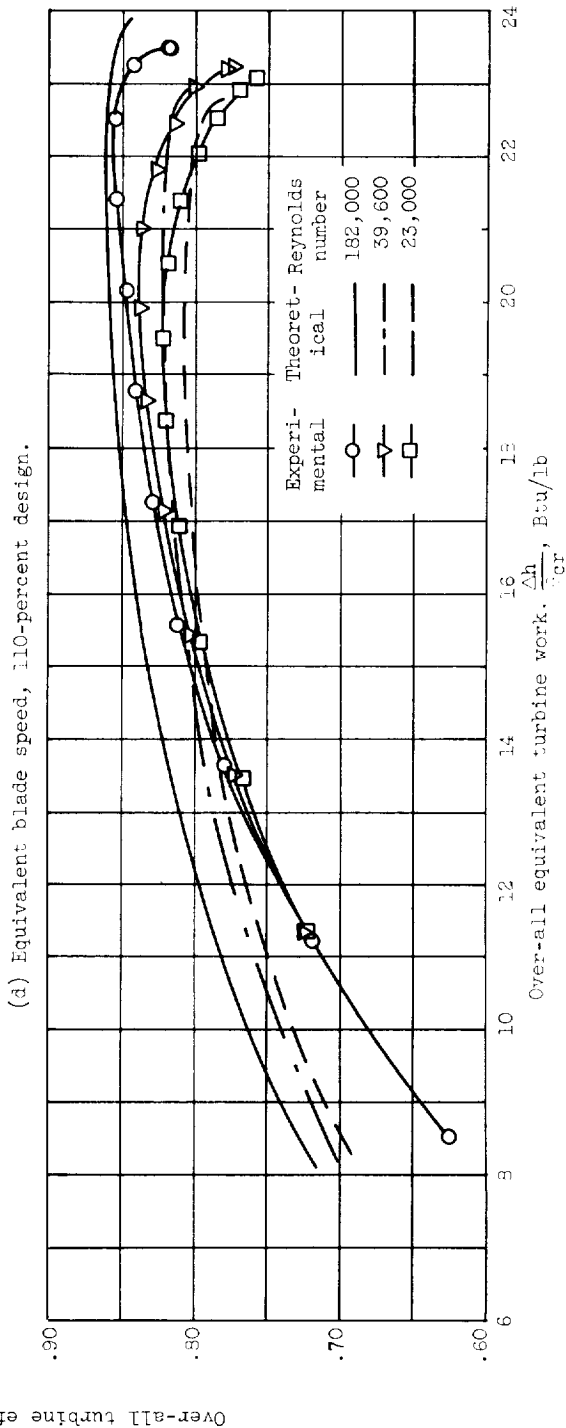
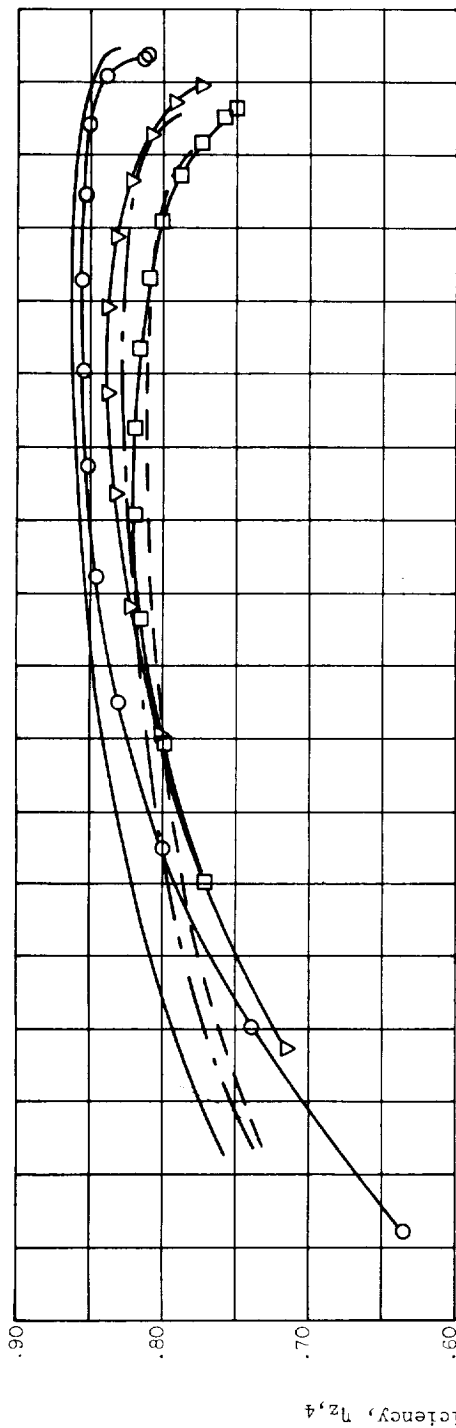


Figure 5. - Concluded. Experimental and theoretical over-all efficiency as a function of equivalent turbine work and Reynolds number.

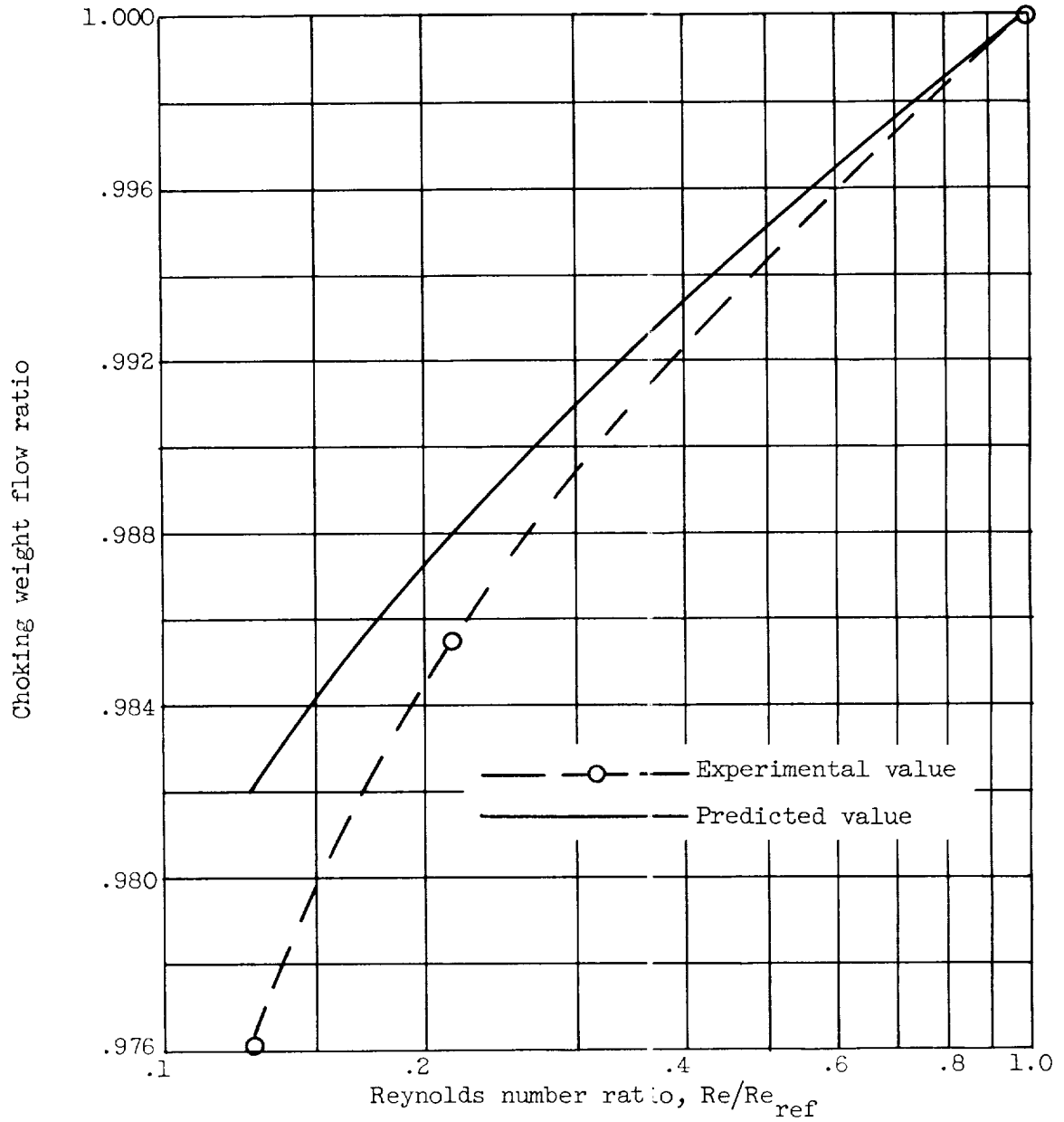


Figure 9. - Turbine choking weight flow as a function of Reynolds number at design speed.

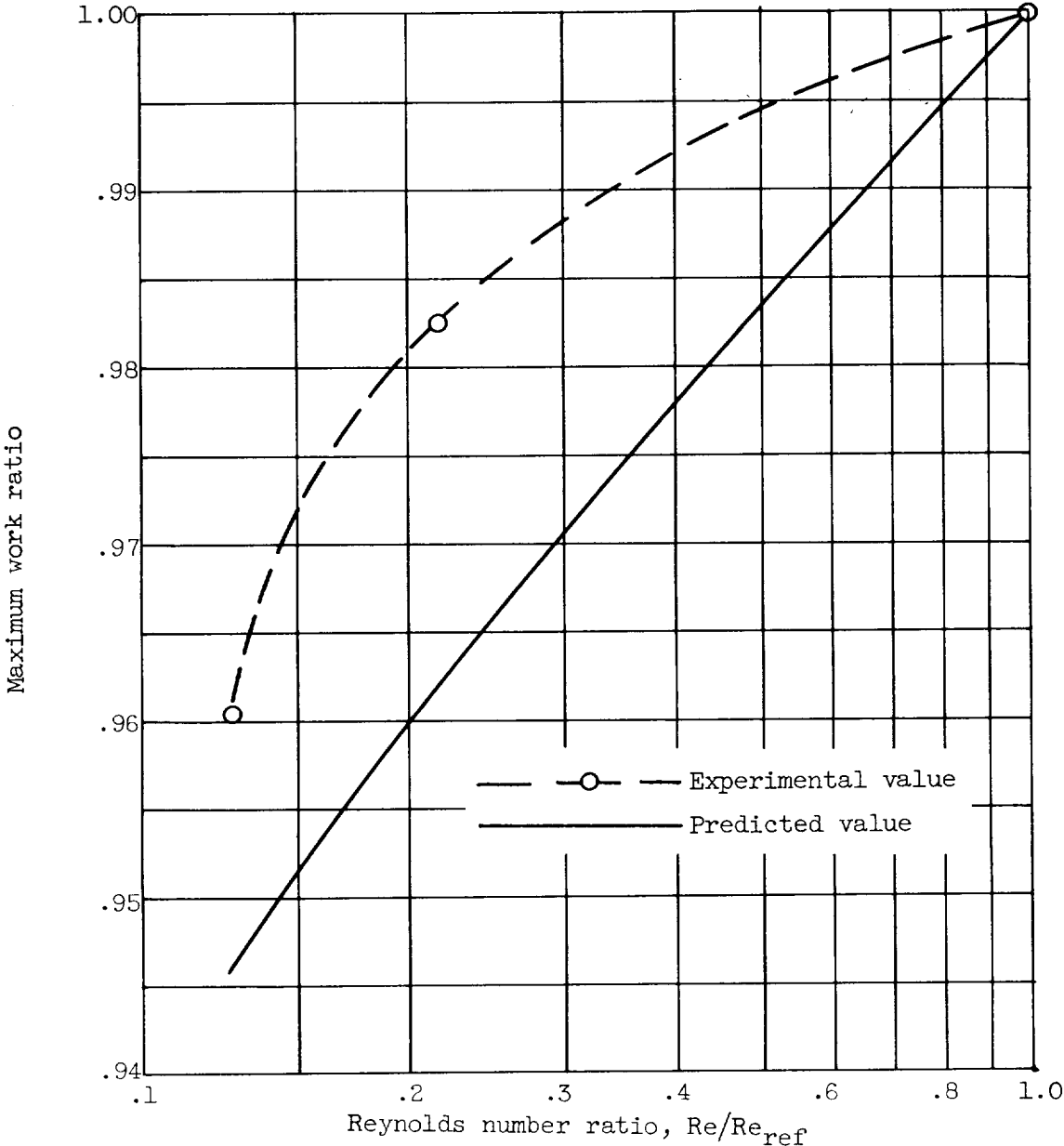


Figure 10. - Maximum turbine work as a function of Reynolds number at design speed.

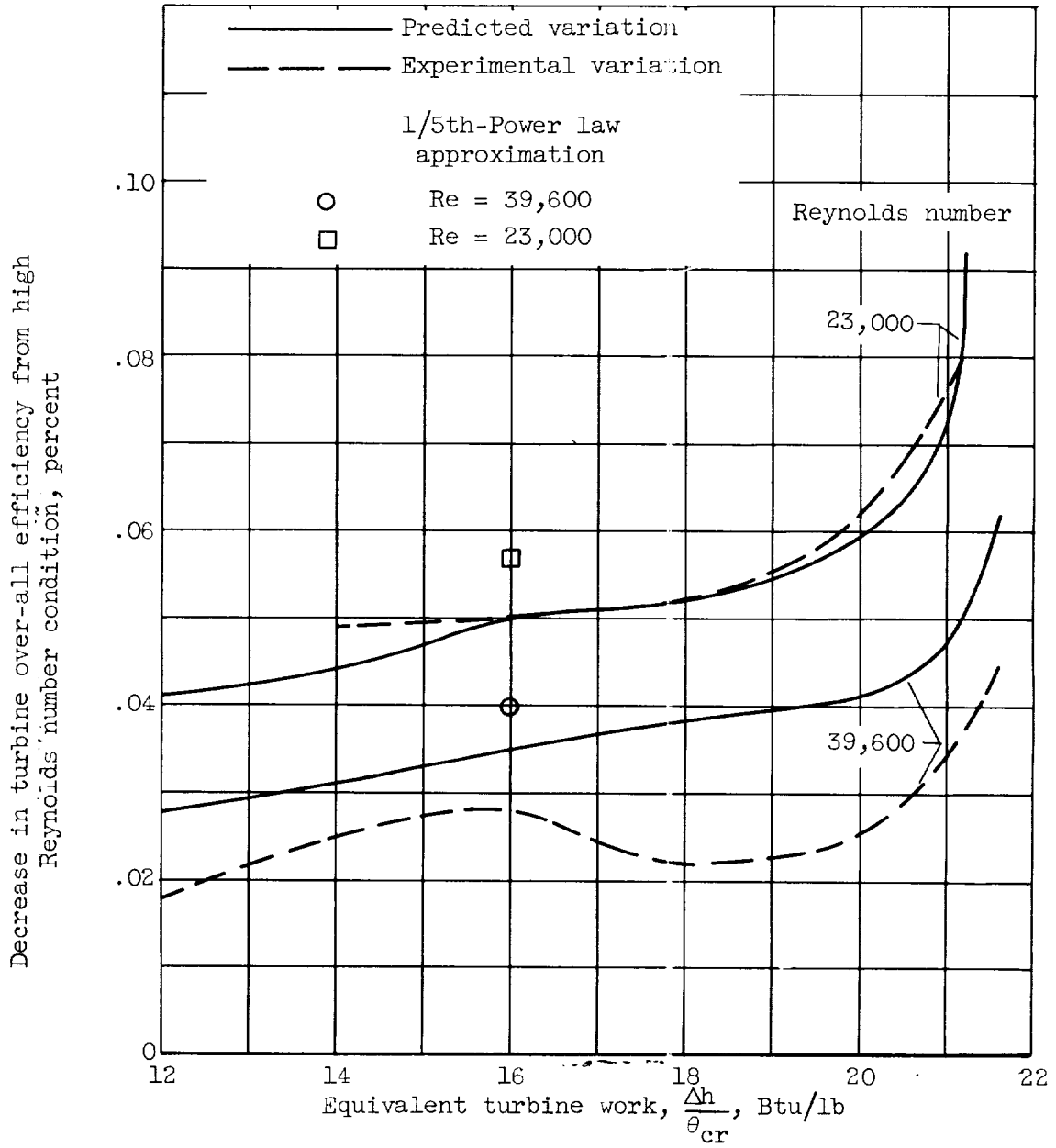
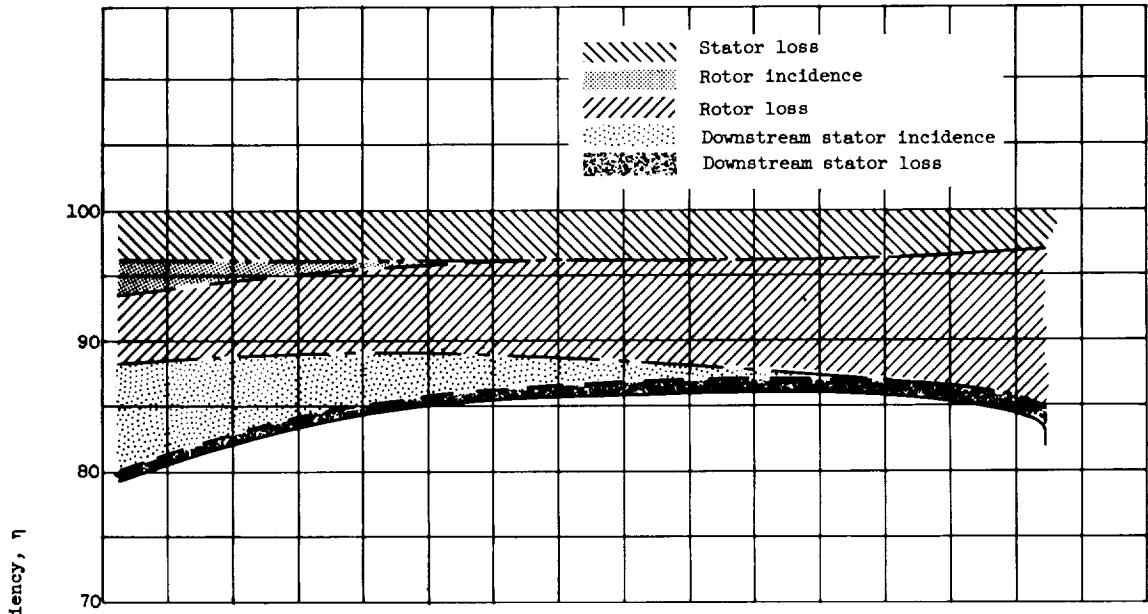


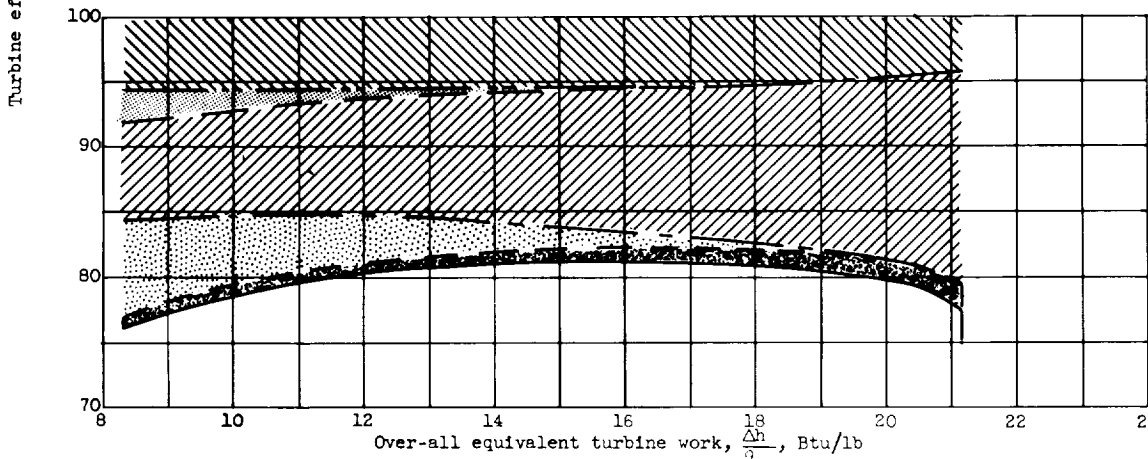
Figure 11. - Change in efficiency as a function of equivalent work and Reynolds number at design rotor speed.



E-185



(a) Reynolds number, 182,500.



(b) Reynolds number, 23,000.

Figure 12. - Effect of various losses on efficiency, 100-percent speed, and Reynolds number indexes, 0.126 and 1.0.



<p>NASA TM X-9 National Aeronautics and Space Administration. INVESTIGATION OF THE EFFECTS OF LOW REYNOLDS NUMBER OPERATION ON THE PERFORMANCE OF A SINGLE-STAGE TURBINE WITH A DOWNSTREAM STATOR. Robert E. Forrette, Donald E. Holeski, and Henry W. Plohr. September 1959. 47p. diags. (NASA TECHNICAL MEMORANDUM X-9)</p> <p>An experimental and analytical investigation of the operation at three Reynolds numbers of a single-stage high-work-output turbine with a downstream stator indicated that deterioration in performance with Reynolds number resulted from increased viscous losses at low Reynolds numbers. An analytical performance prediction method using fundamental boundary-layer relations was used to calculate turbine performance at each Reynolds number. The correlation with experimental results was good provided the</p> <p>(over)</p>	<ol style="list-style-type: none"> <li>1. Engines, Turbojet (3.1.3)</li> <li>2. Turbine Flow Theory and Experiment (3.7.1)</li> <li>3. Turbines - Axial-Flow (3.7.1.1)</li> </ol> <ol style="list-style-type: none"> <li>I. Forrette, Robert E.</li> <li>II. Holeski, Donald E.</li> <li>III. Plohr, Henry W.</li> <li>IV. NASA TM X-9</li> </ol> <p style="text-align: right;">NASA</p>	<ol style="list-style-type: none"> <li>1. Engines, Turbojet (3.1.3)</li> <li>2. Turbine Flow Theory and Experiment (3.7.1)</li> <li>3. Turbines - Axial-Flow (3.7.1.1)</li> </ol> <ol style="list-style-type: none"> <li>I. Forrette, Robert E.</li> <li>II. Holeski, Donald E.</li> <li>III. Plohr, Henry W.</li> <li>IV. NASA TM X-9</li> </ol> <p style="text-align: right;">NASA</p>
<p>NASA TM X-9 National Aeronautics and Space Administration. INVESTIGATION OF THE EFFECTS OF LOW REYNOLDS NUMBER OPERATION ON THE PERFORMANCE OF A SINGLE-STAGE TURBINE WITH A DOWNSTREAM STATOR. Robert E. Forrette, Donald E. Holeski, and Henry W. Plohr. September 1959. 47p. diags. (NASA TECHNICAL MEMORANDUM X-9)</p> <p>An experimental and analytical investigation of the operation at three Reynolds numbers of a single-stage high-work-output turbine with a downstream stator indicated that deterioration in performance with Reynolds number resulted from increased viscous losses at low Reynolds numbers. An analytical performance prediction method using fundamental boundary-layer relations was used to calculate turbine performance at each Reynolds number. The correlation with experimental results was good provided the</p> <p>(over)</p>	<ol style="list-style-type: none"> <li>1. Engines, Turbojet (3.1.3)</li> <li>2. Turbine Flow Theory and Experiment (3.7.1)</li> <li>3. Turbines - Axial-Flow (3.7.1.1)</li> </ol> <ol style="list-style-type: none"> <li>I. Forrette, Robert E.</li> <li>II. Holeski, Donald E.</li> <li>III. Plohr, Henry W.</li> <li>IV. NASA TM X-9</li> </ol> <p style="text-align: right;">NASA</p>	<ol style="list-style-type: none"> <li>1. Engines, Turbojet (3.1.3)</li> <li>2. Turbine Flow Theory and Experiment (3.7.1)</li> <li>3. Turbines - Axial-Flow (3.7.1.1)</li> </ol> <ol style="list-style-type: none"> <li>I. Forrette, Robert E.</li> <li>II. Holeski, Donald E.</li> <li>III. Plohr, Henry W.</li> <li>IV. NASA TM X-9</li> </ol> <p style="text-align: right;">NASA</p>
<p>NASA TM X-9 National Aeronautics and Space Administration. INVESTIGATION OF THE EFFECTS OF LOW REYNOLDS NUMBER OPERATION ON THE PERFORMANCE OF A SINGLE-STAGE TURBINE WITH A DOWNSTREAM STATOR. Robert E. Forrette, Donald E. Holeski, and Henry W. Plohr. September 1959. 47p. diags. (NASA TECHNICAL MEMORANDUM X-9)</p> <p>An experimental and analytical investigation of the operation at three Reynolds numbers of a single-stage high-work-output turbine with a downstream stator indicated that deterioration in performance with Reynolds number resulted from increased viscous losses at low Reynolds numbers. An analytical performance prediction method using fundamental boundary-layer relations was used to calculate turbine performance at each Reynolds number. The correlation with experimental results was good provided the</p> <p>(over)</p>	<ol style="list-style-type: none"> <li>1. Engines, Turbojet (3.1.3)</li> <li>2. Turbine Flow Theory and Experiment (3.7.1)</li> <li>3. Turbines - Axial-Flow (3.7.1.1)</li> </ol> <ol style="list-style-type: none"> <li>I. Forrette, Robert E.</li> <li>II. Holeski, Donald E.</li> <li>III. Plohr, Henry W.</li> <li>IV. NASA TM X-9</li> </ol> <p style="text-align: right;">NASA</p>	<ol style="list-style-type: none"> <li>1. Engines, Turbojet (3.1.3)</li> <li>2. Turbine Flow Theory and Experiment (3.7.1)</li> <li>3. Turbines - Axial-Flow (3.7.1.1)</li> </ol> <ol style="list-style-type: none"> <li>I. Forrette, Robert E.</li> <li>II. Holeski, Donald E.</li> <li>III. Plohr, Henry W.</li> <li>IV. NASA TM X-9</li> </ol> <p style="text-align: right;">NASA</p>
<p>NASA TM X-9 National Aeronautics and Space Administration. INVESTIGATION OF THE EFFECTS OF LOW REYNOLDS NUMBER OPERATION ON THE PERFORMANCE OF A SINGLE-STAGE TURBINE WITH A DOWNSTREAM STATOR. Robert E. Forrette, Donald E. Holeski, and Henry W. Plohr. September 1959. 47p. diags. (NASA TECHNICAL MEMORANDUM X-9)</p> <p>An experimental and analytical investigation of the operation at three Reynolds numbers of a single-stage high-work-output turbine with a downstream stator indicated that deterioration in performance with Reynolds number resulted from increased viscous losses at low Reynolds numbers. An analytical performance prediction method using fundamental boundary-layer relations was used to calculate turbine performance at each Reynolds number. The correlation with experimental results was good provided the</p> <p>(over)</p>	<ol style="list-style-type: none"> <li>1. Engines, Turbojet (3.1.3)</li> <li>2. Turbine Flow Theory and Experiment (3.7.1)</li> <li>3. Turbines - Axial-Flow (3.7.1.1)</li> </ol> <ol style="list-style-type: none"> <li>I. Forrette, Robert E.</li> <li>II. Holeski, Donald E.</li> <li>III. Plohr, Henry W.</li> <li>IV. NASA TM X-9</li> </ol> <p style="text-align: right;">NASA</p>	<ol style="list-style-type: none"> <li>1. Engines, Turbojet (3.1.3)</li> <li>2. Turbine Flow Theory and Experiment (3.7.1)</li> <li>3. Turbines - Axial-Flow (3.7.1.1)</li> </ol> <ol style="list-style-type: none"> <li>I. Forrette, Robert E.</li> <li>II. Holeski, Donald E.</li> <li>III. Plohr, Henry W.</li> <li>IV. NASA TM X-9</li> </ol> <p style="text-align: right;">NASA</p>
<p>NASA TM X-9 National Aeronautics and Space Administration. INVESTIGATION OF THE EFFECTS OF LOW REYNOLDS NUMBER OPERATION ON THE PERFORMANCE OF A SINGLE-STAGE TURBINE WITH A DOWNSTREAM STATOR. Robert E. Forrette, Donald E. Holeski, and Henry W. Plohr. September 1959. 47p. diags. (NASA TECHNICAL MEMORANDUM X-9)</p> <p>An experimental and analytical investigation of the operation at three Reynolds numbers of a single-stage high-work-output turbine with a downstream stator indicated that deterioration in performance with Reynolds number resulted from increased viscous losses at low Reynolds numbers. An analytical performance prediction method using fundamental boundary-layer relations was used to calculate turbine performance at each Reynolds number. The correlation with experimental results was good provided the</p> <p>(over)</p>	<ol style="list-style-type: none"> <li>1. Engines, Turbojet (3.1.3)</li> <li>2. Turbine Flow Theory and Experiment (3.7.1)</li> <li>3. Turbines - Axial-Flow (3.7.1.1)</li> </ol> <ol style="list-style-type: none"> <li>I. Forrette, Robert E.</li> <li>II. Holeski, Donald E.</li> <li>III. Plohr, Henry W.</li> <li>IV. NASA TM X-9</li> </ol> <p style="text-align: right;">NASA</p>	<ol style="list-style-type: none"> <li>1. Engines, Turbojet (3.1.3)</li> <li>2. Turbine Flow Theory and Experiment (3.7.1)</li> <li>3. Turbines - Axial-Flow (3.7.1.1)</li> </ol> <ol style="list-style-type: none"> <li>I. Forrette, Robert E.</li> <li>II. Holeski, Donald E.</li> <li>III. Plohr, Henry W.</li> <li>IV. NASA TM X-9</li> </ol> <p style="text-align: right;">NASA</p>

NASA TM X-9

experimental and analytical design conditions were correctly matched with regard to design performance parameters.

NASA

NASA TM X-9

experimental and analytical design conditions were correctly matched with regard to design performance parameters.

NASA

NASA TM X-9

experimental and analytical design conditions were correctly matched with regard to design performance parameters.

NASA

NASA TM X-9

experimental and analytical design conditions were correctly matched with regard to design performance parameters.

NASA